Electron Spin Resonance Experiments on Shallow Donors in Germanium

D. K. WILSON*
Bell Telephone Laboratories, Whippany, New Jersey
(Received 4 November 1963)

At liquid helium temperatures, spin resonance of localized donor electrons has been observed in phorphorus-, arsenic-, and bismuth-doped germanium. The presence of hyperfine splitting confirms the singlet as the ground state for all three. The separation of the excited triplet states has been measured by uniaxially stressing the samples. The triplet states are all found to lie close to the effective-mass value of 0.009 eV. The anisotropy of the g tensor has also been measured by uniaxial stress measurements giving a value for the g anisotropy $g_{\parallel}-g_{\perp}=-1.05$ for arsenic-doped germanium. The large g anisotropy gives rise to an anisotropic linewidth which is caused by built-in strains in the crystal. Measurements show a strong correlation of this line broadening with the number of dislocations. The broadening is larger than predicted as a result of condensation of the impurities in the neighborhood of dislocations. The linewidth for magnetic fields in the [100] direction, where strain broadening of the line vanishes, has been shown to arise from unresolved hyperfine interactions with Ge^{73} nuclei. The linewidths are in good agreement with values calculated using an isotropic approximation to the effective-mass wave function. The spin-lattice relaxation times have been measured and compared with the theory of Roth and Hasegawa for the one-phonon process. The temperature dependence, the dependence on amplitude and orientation of the magnetic field, and effects of strain predicted by their theory were observed.

I. INTRODUCTION

THE substitution of a column five impurity, such as phosphorus or arsenic for a host atom in germanium or silicon gives rise to energy levels slightly below the conduction band within the forbidden gap. These are called the shallow donor levels.[1] Since the conduction-band minima in both silicon and germanium are not at the center of the Brillouin zone, there are several equivalent conduction band minima. The conduction band is said to be multivalleyed, and as a consequence, the shallow donor levels which split off from the conduction band are degenerate, with a degeneracy equal to the number of valleys. In silicon the degeneracy is sixfold and in germanium, fourfold. The interaction of the localized donor electron and the donor core (called the central cell correction) splits the degenerate donor level into a singlet, doublet, and triplet for silicon and a singlet and triplet for germanium. An effective-mass model of these donor states has been developed by Kohn and Luttinger[2,3] and has been largely confirmed experimentally.

At sufficiently low temperatures, the electrons become localized about the donor sites. Electron spin resonance[4] for such unpaired donor electrons in silicon was first observed by Fletcher and his co-workers.[5] The resonance spectrum was found to consist of $2I+1$ lines arising from the hyperfine interaction of the donor electron and the donor nucleus, where I is the nuclear spin of the donor atom. The study of this spectrum has yielded much valuable information about the donor states and the band structure of silicon.[6–8] The obvious extension of the technique to germanium was attempted soon after the initial discoveries but the initial search for spin resonance of germanium donors was unsuccessful for a number of reasons. The most important of these results from the fact that the binding energy of the donor electrons is rather small in germanium. This means that the effective orbit of these electrons is very large. If the electrons in neighboring donors are not to interact, then the maximum allowable concentration of donors is rather small. This, in turn, reduces the available signal-to-noise ratio for germanium donor electrons appreciably.

The resonance spectra in silicon was consistent with the assignment of the singlet to the lowest state for all the donors. The evidence that the singlet was the ground state in germanium was indirect and in view of the failure to observe donor spin resonance was subject to some doubt. In order to resolve this question and to obtain information about the donor states, we undertook another search for the donor electron resonance in germanium.

In this paper we will first review the nature of the donor electron spin resonance in germanium (Sec. II) and, since the early experiments showed pronounced effects due to mechanical stress, we also will discuss the changes in the resonance spectrum under stress (Sec. III). In subsequent sections we present details of the experimental method (Sec. IV) and the experimental results both in unstressed samples (Sec. V) and stressed samples (Sec. VI). These experimental results are summarized in the remainder of this section.

* This work was performed in partial fulfillment of the requirements for a Ph.D. degree at Rutgers, The State University, New Brunswick, New Jersey.

[1] For a review of donor states, see W. Kohn, in *Solid-State Physics*, edited by F. Seitz and D. Turnbull (Academic Press Inc., New York, 1957), Vol. 5.

[2] W. Kohn and J. M. Luttinger, Phys. Rev. **97**, 1721 (1955).

[3] W. Kohn and J. M. Luttinger, Phys. Rev. **98**, 915 (1955).

[4] For a review of spin resonance in semiconductors, see G. W. Ludwig and H. H. Woodbury, in *Solid-State Physics*, edited by F. Seitz and D. Turnbull (Academic Press Inc., New York, 1962), Vol. 13.

[5] R. C. Fletcher, W. A. Yager, G. L. Pearson, and F. R. Merritt, Phys. Rev. **95**, 844 (1954).

[6] G. Feher, Phys. Rev. **114**, 1219 (1959).

[7] G. Feher and E. Gere, Phys. Rev. **114**, 1245 (1959).

[8] D. K. Wilson and G. Feher, Phys. Rev. **124**, 1068 (1961).

In rather lightly doped germanium, we were able, at 4.2°K, to observe the spin resonance of localized donor electrons for arsenic, phosphorus, antimony, and bismuth donors in germanium.[9] The g values all differ markedly from the free electron value; a consequence of the strong spin-orbit interaction of conduction electrons with the host germanium nuclei. The hyperfine splittings observed establish the singlet as the ground state for arsenic-, phosphorus-, and bismuth-doped germanium. Antimony-doped samples yielded a variety of results which indicated that the triplet was very close to the singlet if not below it. The magnitude of the hyperfine splitting is determined by the probability amplitude of the donor electron at the impurity nucleus. In germanium, as in the case of silicon, this probability amplitude deviates appreciably from the effective-mass calculation. This is to be expected since the effective-mass wave function cannot be considered valid in the vicinity of the donor nucleus.[1]

The hyperfine lines in all cases were broad, the broadening being very anisotropic. The minimum linewidth always occurred when the magnetic field was along the [100] crystal axis. This minimum linewidth is due to unresolved hyperfine interactions with Ge^{73} nuclei. This mechanism has been confirmed by the observation of a much narrower line in a sample with reduced concentration of Ge^{73}. The magnitude of the broadening can be calculated using the effective-mass wave function in the region outside the donor nucleus. Using an isotropic approximation to the effective-mass wave function, we have obtained values for the spread of the wave function which are in good agreement with effective mass values for phosphorus-, arsenic-, and bismuth-doped germanium.

The g shift with strain, which was also observed to a much smaller degree in silicon,[8] is due to the multivalleyed nature of the conduction band. Strain shifts the relative energies of the different valleys and causes certain of the valleys to be preferred. Since the single-valley g values are highly anisotropic, the g shifts under strain. From the application of uniform uniaxial stress and the consequent changes in the resonance spectrum, we have been able to determine the anisotropy in the single-valley g values. The observed values are in rough agreement with those calculated by Laura Roth[10] using a two-band model, although some discrepancy has been pointed out by Liu.[11]

Since the states that are mixed into the singlet ground state by strain are the triplet states which have no hyperfine interaction, it has also been possible to determine the position of the triplet from the changes in the hyperfine splitting with strain. From such measurements we have determined the singlet-triplet splitting for phosphorus, arsenic, and bismuth donors in germanium. The location of the triplet with respect to the conduction band is in very good agreement with the calculated value of 0.009 eV for all donors in germanium. In the case of antimony donors, the very small value of the splitting between singlet and triplet[12] causes the resonance spectrum to be unusually sensitive to lattice imperfections.

In Sec. VII of this paper we discuss the relationship of these strain experiments to the spin-lattice relaxation of donor electrons and the results of measurements of relaxation times in germanium. Roth[10] and Hasegawa[13] have shown that an important mechanism for relaxing the electron spin arises if the g values are strain sensitive. That is, the time-varying strain due to a phonon will, in effect, produce a time-varying magnetic field because it modulates the g value. The magnitude of this effect is related to the anisotropy of the single-valley g value and to the splitting of the singlet and triplet. Using the values obtained in this work, a relaxation time for germanium donors of the order of 10^{-3} sec at liquid helium temperatures is expected for this mechanism. In order to check this calculation, a study of the spin relaxation time was made in arsenic-doped germanium. The observed values were in good agreement with the Roth-Hasegawa theory. Both the linear temperature dependence and quartic field dependence characteristic of a single phonon process were observed. In addition, both the predicted angular dependence and the change in relaxation rate for a sample under strain were noted.

In Sec. VIII we discuss the experimental results at high-impurity concentrations, where the wave functions of adjacent impurities begin to overlap and the donor electron can hop from site to site. That is, the electrons become "nonlocalized." If the hopping frequency is high enough, the local hyperfine interactions are averaged out and a single narrow line is observed. The initial effects of hopping are noted at a donor concentration of $5\times10^{15}/cm^3$ in arsenic-doped germanium and $10^{15}/cm^3$ in phosphorus-doped germanium; the difference arising from the difference in binding energy of the two. The linewidth of the nonlocalized resonance lines and their temperature dependence is in agreement with the impurity conduction model proposed by Miller and Abraham.[14] The g values for such nonlocalized electrons are very close to those for the localized ones, which implies that the hopping electrons spend most of the time trapped in a donor orbit. Uniaxial strain which strongly effects the wave functions and hence, the hopping time, not only shifts the line but markedly affects its width. These effects will also be discussed.

---

[9] G. Feher, D. K. Wilson, and E. Gere, Phys. Rev. Letters **3**, 25 (1959).
[10] L. Roth, Phys. Rev. **118**, 1534 (1960).
[11] L. Liu, Phys. Rev. **126**, 1317 (1962).
[12] H. Fritzsche, Phys. Rev. **120**, 1120 (1960).
[13] H. Hasegawa, Phys. Rev. **118**, 1523 (1960).
[14] A. Miller and E. Abraham, Phys. Rev. **120**, 745 (1960).

II. STRUCTURE OF THE DONOR STATES IN THE ABSENCE OF EXTERNAL STRESS

A. Wave Function

We wish to review briefly the nature of the donor ground state, first in the unstrained crystal and then in a crystal subjected to uniaxial stress.[1]

The loosely bound donor electron is treated in the effective-mass approximation as a hydrogen-like atom where the Coulomb attraction of the donor core is reduced by the dielectric constant of the semiconductor host and the electron is assumed to move with the effective mass of a conduction-band electron. Then, in effective-mass theory, the wave function for the localized donor electron wave function is a product of the conduction-band Bloch function and the solution of the Schroedinger equation for the hydrogen-like atom formed by the donor and its loosely bound electron.

As we have pointed out, the conduction-band minima in germanium is not at the center of the zone, but is at the zone edge in a [111] direction. There are, therefore, four equivalent minima. Since the donor electron can select a wave function equally well from any of the minima, the complete donor wave function is of the form:

$$\psi(r)=\sum_{j=1}^{4}\alpha_j F^j(r)u^j(r)e^{i\mathbf{k}_j\cdot\mathbf{r}}, \tag{1}$$

where $u^j(r)$ is the conduction-band wave function at the jth minima, $F^j(r)$ is the hydrogenic envelope function, and α_j describes the relative contribution from the jth valley. A further complication arises in the envelope function because the effective masses vary with the direction of electron motion; the wave function is thus no longer spherical but becomes compressed in the direction of the heavier mass. For germanium, where $m_{\parallel}=1.60$ and $m_{\perp}=0.08$,[1] $F^j(r)$ becomes pancake shaped with the axis pointed in the [111] direction. In forming the sum over the four valleys, the total wave function is more or less spherical.

For this anisotropic case, Kohn and Luttinger[2,15] have used a trial wave function of the form

$$F^j(r)=(\pi a^2 b)^{-1/2}\exp\{-[(x_j^2+y_j^2)/a^2+z_j^2/b^2]^{1/2}\}, \tag{2}$$

where z_j is the displacement along the jth valley axis, $(x_j^2+y_j^2)^{1/2}$ is the perpendicular distance from it and a and b are the effective Bohr radii in the transverse and parallel directions, respectively.

A variational calculation for the transverse and parallel effective radii gives the values $a=64.5$ Å, $b=22.7$ Å for any donor in germanium and an ionization energy, $E_{\text{eff mass}}=0.0092$ eV. Since the lattice constant of germanium is 5.66 Å, we see that the donor wave function spreads effectively over hundreds of lattice sites. In order to ensure that no overlap of adjacent donor wave functions occurs, it is necessary to restrict the impurity concentration so that the average impurity spacing is greater than $10(a^2b)^{1/3}$.[16] This limits us to maximum impurity concentrations of the order of $10^{15}/\text{cm}^3$. On the other hand, in silicon the wave functions are more compressed and the maximum impurity concentration is between one and two orders of magnitude larger. Therefore, we expect a considerably weaker spin resonance signal in germanium than in silicon.

The ground-state wave functions for germanium can be arranged in terms of the contribution from the jth valley (α_j) as follows: A singlet state which is nonvanishing at the origin

$$\alpha_j=\tfrac{1}{2}(1,1,1,1), \tag{3}$$

and a triplet of levels which vanish at the origin

$$\begin{aligned}&\text{(a)}\quad \alpha_j=\tfrac{1}{2}(1,1,-1,-1);\\ &\text{(b)}\quad \alpha_j=1/\sqrt{2}(1,-1,0,0);\\ &\text{(c)}\quad \alpha_j=1/\sqrt{2}(0,0,1,-1);\end{aligned} \tag{4}$$

(the particular representation of the levels chosen here will be of use in the later discussion of the effects of a stress applied in the [110] crystallographic direction). It can be shown that no tetrahedrally symmetric perturbation can lift the triplet degeneracy. As noted, the quantity $|\psi_{(0)}|^2$ will be large for the singlet, whereas it vanishes for the triplet states. We expect the effective-mass approximation in the neighborhood of the donor core to break down. Since the electron probability density does not vanish at the donor nucleus for the singlet, this deviation from effective-mass approximation should lift the singlet-triplet degeneracy. The resultant splitting of the singlet and triplet we shall refer to as the valley-orbit splitting,[17] since the treatment of the effect is analogous to that for the spin-orbit splitting. In the case of silicon, the ground state has been confirmed as the singlet from the observed hyperfine spectrum and the splitting of the excited states has been measured from the effects of uniaxial stress on the resonance spectrum.[8] We will discuss the application of this technique to germanium as well. First, however, let us consider in more detail the nature of the hyperfine spectrum.

B. Spin Hamiltonian

Magnetic interactions of the magnetic moment of the donor electron $\boldsymbol{\mu}_e$, the nuclear moment of the donor $\boldsymbol{\mu}_D$, the nuclear moment of the Ge^{73} $\boldsymbol{\mu}_{Ge}$, which also interact with the donor electron, and the magnetic field $\mathbf{H}$ give rise to the following Hamiltonian:

$$\mathcal{H}=-\boldsymbol{\mu}_e\cdot\mathbf{H}+\frac{8\pi}{3}\boldsymbol{\mu}_e\cdot\boldsymbol{\mu}_D|\psi_{(0)}|^2+\frac{8\pi}{3}\boldsymbol{\mu}_e\cdot\sum_l\boldsymbol{\mu}_{Ge}|\psi(r_l)|^2, \tag{5}$$

[15] M. Lampert, Phys. Rev. **97**, 352 (1955).

[16] E. Conwell, Phys. Rev. **103**, 51 (1956).

[17] G. Weinreich and H. G. White, Bull. Am. Phys. Soc. **5**, 60 (1960).

where we assume that the wave function has cubic symmetry and we neglect the interaction of the nuclear moments with the magnetic field.

If we assume the donor electron orbit is more or less S-like, then the energy levels for this Hamiltonian are

$$E=g\beta Hm_S+\frac{16\pi}{3}\beta\frac{\mu_D}{I_D}|\psi(0)|^2m_Sm_D + \frac{16\pi}{3}\beta\frac{\mu_{Ge}}{I_{Ge}}m_S\sum_l|\psi(r_l)|^2m_l; \quad (6)$$

m_S, m_D,m_l are magnetic quantum numbers for the electron, donor nucleus, and Ge^{73} nucleus, respectively, g is the electronic g value, and β is the Bohr magneton. An electromagnetic field of frequency ν induces resonance transitions with $\Delta m_S=\pm1$, $\Delta m_D=0$, $\Delta m_l=0$, so that

$$h\nu=g\beta H+\frac{16\pi}{3}\beta\frac{\mu_D}{I_D}|\psi(0)|^2m_D + \frac{16\pi}{3}\beta\frac{\mu_{Ge}}{I_{Ge}}\sum_l|\psi(r_l)|^2m_l. \quad (7)$$

Since there are $2I+1$ values for m_D, there are $2I+1$ values of the magnetic field at which resonance is observed. For this hyperfine spectrum, adjacent values of the field are separated by[18]

$$\Delta H_{\rm hfs}=(16\pi/3g)|\psi(0)|^2. \quad (8)$$

Each of the Ge^{73} hyperfine interactions gives rise to a similar field shift whose total effect is given as the sum

$$M_2=\frac{16\pi}{3g}\frac{\mu_{Ge}}{I_{Ge}}\sum_l|\psi(r_l)|^2m_l. \quad (9)$$

The first moment of this sum vanishes but its second moment gives rise to a broadening of the line. We will consider this term in more detail later.

Using the effective-mass wave function [Eq. (1)] and the valley populations [Eqs. (3), (4)] for germanium, we find that

$$\text{singlet} \quad |\psi(0)|^2=4|F_{(0)}|^2\eta_{Ge}, \quad (10)$$

$$\text{triplet} \quad |\psi(0)|^2=0, \quad (11)$$

where the quantity $\eta_{Ge}=|u(r_l)|^2$ is proportional to the probability amplitude for the conduction-band electrons at the lattice sites. The presence of a hyperfine spectrum of measurable splitting is, therefore, an absolute test of the nature of the donor ground state.

The bunching of the Bloch functions at lattice sites (η_{Ge}) is not known for germanium. We have made an experimental estimate based on observed nuclear spin-lattice relaxation times which indicates η_{Ge} is an order of magnitude larger than η_{Si}. This is to be expected in view of the larger nuclear charge for germanium. We will see that several of the differences in the spin resonance spectrum of germanium donors and silicon donors arise from this pronounced bunching up of Bloch functions at the germanium sites.

In the case of the triplet state the absence of hyperfine splitting does not assure that the spectrum will reduce to a single line. It has been pointed out by Keyes and Price[19] that the triplet degeneracy could be lifted by local strains in the crystal. In the extreme, this could lead to a state where the donor electrons occupied one valley in a given region of the material and another valley in some other region of the crystal. This would give rise to a spectrum of four lines following the valley symmetry and exhibiting principal g values corresponding to the single valley values. In the more usual case where the strains are perfectly random, the spectrum for the triplet would consist of a wide distribution of resonances and would then be essentially wiped out. This could be the case for antimony-doped germanium. A similar effect occurs in the case of acceptors in silicon and is overcome in that case by applying a large uniform strain to minimize the effects of the localized ones.[20]

C. Linewidth

The last term in the spin Hamiltonian arises from the hyperfine interactions of the donor electron with the Ge^{73} isotope. The isotopic abundance is 7.8% and its spin is $\frac{9}{2}$. In the average donor orbit, therefore there will be interactions with hundreds of such randomly located nuclei, each having 10 possible nuclear orientations. The resulting average magnetic field that each donor electron sees will vary from site to site with just as many sites having fields higher than the applied magnetic field as sites having lower fields. Thus, this term does not shift the resonance, it merely broadens it. This "inhomogeneous" broadening can be calculated using the assumed ground-state wave function appropriately corrected for the ionization energy of the donor involved. Following Kohn's calculation for silicon,[21] the second moment of the line (M_2) is given by

$$M_2^2=\left(\frac{16\pi}{3g}\frac{\mu_{Ge}}{I_{Ge}}\right)^2\sum_l\sum_i|\alpha_ju^j(r_l)e^{i\mathbf{k}_j\cdot\mathbf{r}_l}F^j(\mathbf{r}_l)|^4m_l^2f, \quad (12)$$

where f is the fractional abundance of Ge^{73}, and we insert the effective-mass wave function for the singlet. Expanding, we obtain for the linewidth ΔH (i.e., the

[18] Y. Yafet [Phys. Chem. Solids **21**, 99 (1961)] has pointed out that the observed g must appear in Eq. (8). Neglect of this fact leads to erroneous values for $|\psi_{(0)}|^2$ given in our original paper (Ref. 9).

[19] R. W. Keyes and P. J. Price, Phys. Rev. Letters **5**, 473 (1960).

[20] G. Feher, J. Hensel, and E. Gere, Phys. Rev. Letters **5**, 309 (1960).

[21] W. Kohn (unpublished).

magnetic-field splitting of the absorption half-maxima).

$$\Delta H_{\mathrm{Ge}^{73}}=2M_2=\frac{32\pi}{3g}\frac{\mu_{\mathrm{Ge}}}{I_{\mathrm{Ge}}}\langle m_l^2\rangle_{\mathrm{av}}{}^{1/2}\times f^{1/2}\frac{\eta}{4}\sum_l n_l|e^{i\mathbf{k}_j\cdot\mathbf{r}_l}F^j(\mathbf{r}_l)|^4, \quad (13)$$

when n_l is the number of equivalent lattice points. The evaluation of the lattice sum is given in the Appendix using an isotropic approximation for $F(r)$ given by Kohn.[1] In this approximation Kohn assumes some average radius $[a^*=(a^2b)^{1/3}]$ of the actual effective-mass radii and, in addition, modifies this radius $(a_0^*=(E_{\text{eff mass}}/E_{\text{obs}})^{1/2}a^*)$ to account for the differences between observed ionization energies (E_{obs}) and the effective-mass value. This approximation gives a calculated linewidth;

$$\Delta H_{\mathrm{Ge}^{73}}=\frac{36}{3g}\frac{\mu_{\mathrm{Ge}}}{I_{\mathrm{Ge}}}\langle m_l^2\rangle_{\mathrm{av}}{}^{1/2}f^{1/2}\eta\frac{1}{a_l^{3/2}a_0^{*3/2}}, \quad (14)$$

where a_l is the lattice constant and a_0^* is therefore an effective Bohr radius related to the spread of the donor wave function. The magnitude of the linewidth is seen to be related to the spread of the wave function and in this sense the observed linewidths are a check on the effective-mass wave functions in the region far away from the donor nucleus whereas the hyperfine splitting of the lines is determined by the magnitude of the wave function at the nucleus.

We see that the linewidth in germanium should be larger than that in silicon, principally because η is appreciably larger in germanium than in silicon. This larger linewidth will also result in a reduced resonance signal amplitude for germanium as compared with silicon.

III. EFFECT OF STRAIN ON THE DONOR STATES

A. Wave Function

The application of external or internal strain[22] destroys certain symmetries of the crystal and alters the ground-state wave function. The strain will depress some of the valleys in energy and raise others; the magnitude of the shift is of the order of $\Xi_\mu s$ where Ξ_μ is the appropriate deformation potential and s is the lattice strain.[23] Under such strain the relative probability of finding the donor electron in the lowered valleys increases at the expense of those in the raised valleys. We have previously called this repopulating the valleys.[8] To look at this change in another fashion, the strain admixes some of the excited triplet state into the singlet ground state so that the electrons favor wave functions from the lowest valleys, the extent of the admixture depending on the quantity $\Xi_\mu s/E_{13}$ where E_{13} is the singlet-triplet splitting. Any strain at all gives rise, therefore, to a new ground state.

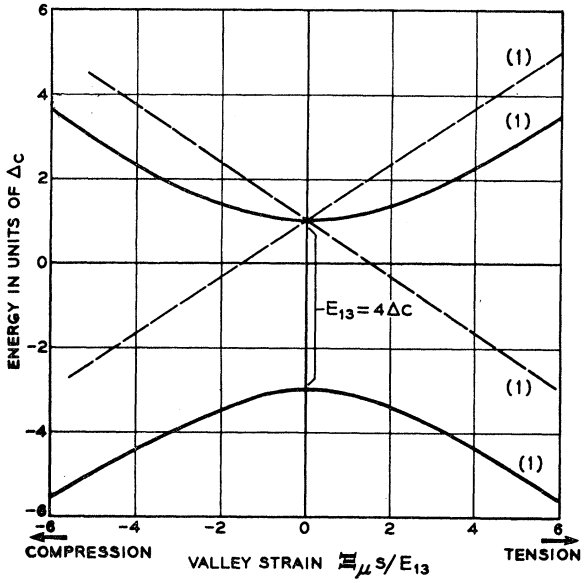

FIG. 1. Energy of the 1s-like donor levels in germanium as a function of the valley strain $\Xi_\mu s/E_{13}$. Energies expressed in units of $\Delta_c=\frac{1}{4}$ {singlet-triplet splitting (E_{13})}.

Consider the effect of a uniaxial compressive stress applied along the [110] direction. There are two valleys lying in a plane containing the stress axis whose energies are equally lowered by the compression. The remaining two lie in a plane at right angles and their energies are raised by the compression. At sufficiently large strains, only the two lowered valley wave functions would contribute to the donor ground state. The energy shifts of the ground state and triplet state under such uniaxial compression are calculated in the Appendix and the results (Fig. 1) show that the triplet state having the valley composition given by Eq. (4a) is mixed into the singlet state by a [110] stress to form the new ground state.

B. Hyperfine Splitting with Strain

Since the triplet wave functions vanish at the donor nucleus, any admixture of these hyperfineless states will reduce the observed hyperfine splitting of the singlet ground state. The change can be expressed as the ratio of the hyperfine splitting with strain to that without. This quantity can be calculated using the effective-mass expression for the wave function and assuming that the only effect of the strain is to change the relative valley populations. This assumption is confirmed by the work of Fritzche.[24] The result for a uniaxial compression along

[22] For a review of strain effects in semiconductors see R. Keyes, in *Solid-State Physics*, edited by F. Seitz and D. Turnbull (Academic Press Inc., New York, 1962), Vol. II.

[23] P. J. Price, Phys. Rev. **104**, 1223 (1956).

[24] H. Fritzsche, Phys. Rev. **125**, 1560 (1962).

a [110] direction is (this calculation is given in Appendix A):

$$\text{hfs}_{\text{strain}}/\text{hfs}_{\text{no strain}}=\tfrac{1}{2}[1+(1+x^2/9)^{-1/2}], \quad (15)$$

where the "valley strain" $x=\Xi_\mu s/E_{13}$. In the limit of very large strains, we find that the hyperfine splitting is reduced to $\frac{1}{2}$ its original value. If the compressive stress were applied in the [111] direction we would expect the single valley in the direction of the stress axis to be lowered and the other three to be raised. In the limit of large strains for this case, the hyperfine splittings would be reduced to $\frac{1}{4}$ its original value. From the measured changes in hfs under uniaxial stress, we will find it possible to obtain the singlet-triplet splitting in germanium[25] as we found the singlet-doublet splitting in silicon.[8]

C. Effects of Strain on g Shift

The first term in the expression for the energy of resonance transitions [Eq. (7)] is $g\beta H$, where the g value is a measure of the interaction of the electron spin angular momentum and its orbital angular momentum. Since the effective mass of the electron varies with the direction of its motion, so, also, will the g value. This is expressed for the case of the electron occupying a single valley in terms of $g_{\parallel}$, the g value for magnetic field parallel to the valley axis and $g_{\perp}$, for the field perpendicular. Then, for arbitrary angle of the magnetic field to the valley axis (Φ), the single-valley g value is given by

$$g^2=g_{\parallel}^2\cos^2\Phi+g_{\perp}^2\sin^2\Phi. \quad (16)$$

In the ground state all four valleys contribute equally and the g, averaged over the four, gives the isotropic result

$$g=g_0=g_{\parallel}/3+2g_{\perp}/3. \quad (17)$$

Roth[10] has calculated the values of $g_{\parallel}$ and $g_{\perp}$ assuming that the dominant contributions to the shift from $g=2$ arise from the valence band which is largely p-like in character and has the smallest energy separation from the conduction band. Since similar arguments apply to the calculation of the effective masses, she finds a relationship between the two for this two-band calculation of the form

$$(g_{\parallel}-2)=-(\delta/E_{cv})(m/m_{\perp}-1), \quad (18)$$
$$(g_{\perp}-2)=-(\delta/E_{cv})(m/m_{\parallel}-1),$$

where δ is the spin-orbit splitting of the valence band edge at the [111] zone boundary and E_{cv} is the energy of the direct transition from that point to the conduction minimum. The large anisotropy in the g's follows from the large-mass anisotropy. Values for both the quantities δ and E_{cv} have been obtained by Tauc and Antoncik[26] from ultraviolet reflectivity measurements and are $\delta=0.18$ eV and $E_{cv}=2.1$ eV. Using the effective-mass values $m_{\perp}=0.08$ and $m_{\parallel}=1.60$, the calculated g's are $g_{\perp}=2.07$ and $g_{\parallel}=0.98$.

In the extremes of strain noted above ($x\gg1$), the g would be highly anisotropic. Thus, for a large compression in the [111] direction, only one valley is populated and the g would vary from $g_{\parallel}$ to $g_{\perp}$. For the large [110] compression, two valleys are occupied and the variation is not quite so large, varying from g_0 to $g_{\perp}$. For small stresses in the [110] direction and small angles to the [100] axis, the g can be expressed in terms of the angle (θ) between the magnetic field and the [100] axis perpendicular to the stress axis (see Appendix B).

$$g-g_0=-\sin^2\theta[4\alpha_1^2-1](g_{\parallel}-g_{\perp})/3g_0, \quad (19)$$

where α_1^2 is the occupation probability of one of the depressed valleys. It is the large value for the term $(g_{\parallel}-g_{\perp})$ in germanium that leads to many of the striking differences between the spin resonance of donors in silicon and germanium.

In this result, note that the g shift for this strain vanishes in the [100] direction. Simply put, this happens because the field makes equal angles with all the valley axes, hence, the relative population of the valleys is irrelevant and the g is affected by strain only in second order.

D. Effect of Strain on the Linewidth in [100] Direction

Just as strain modifies the hyperfine interaction of the donor electron with the donor nucleus through changes in the ground-state wave function, so also will changes occur in the interaction with the Ge^{73} nuclei. The principal effect is again that of valley repopulation. Since the linewidth also depends on the number of occupied valleys. [see Eq. (12) in Sec. III, C] a large compressive stress in the [110] direction would be expected to reduce the linewidth by $\frac{1}{2}$. Fritzsche[24] has pointed out that the envelope part ($F(r)$) of the ground-state wave function also changes with strain because the admixing of triplet states which have no central cell correction will cause the effective donor orbit radius $(a^2b)^{1/3}$ to increase. The effect on the donor hyperfine splitting is small but that on the unresolved Ge^{73} interactions will be comparable to that from the valley repopulation. We estimate for arsenic donors that this effect should further reduce the linewidth for large stresses by 15%.

The decrease in linewidth is experimentally observed; however, it is smaller than that expected from the valley repopulation. This is a result of inhomogeneous strain. Any gradient in strain will give rise to a distribution in donor nucleus hyperfine splittings so that the linewidth is increased by such inhomogenieties. In the extreme of a large [111] strain where ultimately only one valley is occupied, the broadening effects of strain gradients should vanish and the linewidth should be reduced

[25] D. K. Wilson and G. Feher, Bull. Am. Phys. Soc. 5, 60 (1960).
[26] J. Tauc and E. Antoncik, Phys. Rev. Letters 5, 253 (1960).

significantly from that observed in an unstrained sample. This effect could possibly be used to improve the signal-to-noise ratio.

E. Effect of Strain on Linewidth Off [100] Direction

In addition to this line broadening term, another contribution occurs when the magnetic field deviates from the [100] crystal axis. As we have pointed out, strains either external or internal for such field directions will produce a shift in the center of the resonance spectrum. Internal strains in single crystals are found to arise in the neighborhood of imperfections and are most severe near dislocations. Since these strains are random in orientation and in magnitude, they give rise to a distribution of possible g values centered about the isotropic value and, hence, to a broadening of the line rather than a shift of its center. Such a contribution to the linewidth is observed in germanium. Although one also observes g shifts with uniaxial stress in silicon, no comparable contribution to the linewidth in silicon is observed, a consequence of the fact that $(g_{\parallel}-g_{\perp})$ is 3 orders of magnitude smaller in silicon.

The increase of the linewidth due to this effect can be estimated as follows. We assume a Gaussian strain distribution with an average component Δs in an arbitrary [111] direction. We neglect the other components as their effects are all smaller than the [111] component for small angles θ between H and [100] axis. In Appendix B, we have calculated the effect of a uniaxial stress in the [111] direction on the g value. For small strains this reduces to

$$\Delta g=\frac{(g_{\parallel}-g_{\perp})}{3g_0}\frac{2}{9}\frac{\Xi_{\mu}\Delta s}{E_{13}}(\sin^2\theta+\sqrt{2}\sin 2\theta), \qquad (20)$$

where θ is angle to the [100] direction. We can write the total linewidth ΔH_T as

$$(\Delta H_T)^2=(\Delta H_{\mathrm{Ge}^{73}})^2+\left(\frac{\Delta g}{g_0}H\right)^2. \qquad (21)$$

Substituting from above,

$$(\Delta H_T)^2=(\Delta H_{\mathrm{Ge}^{73}})^2+\left\{\frac{g_{\parallel}-g_{\perp}}{3g_0^2}H-\frac{2}{9}\frac{\Xi_{\mu}\Delta s}{E_{13}}\right\}^2(\sin^2\theta+\sqrt{2}\sin 2\theta)^2. \qquad (22)$$

The linewidth will be a minimum in [100] and a maximum in the [111] direction. (As the magnetic field approaches [110] direction, the linewidth should decrease; however, in this direction the broadening due to strain components in the [110] direction will also become important. The detailed behavior for large angles will depend on the relative amplitudes of the resolved strain components about the dislocations.) We see that the effect of this strain broadening on the linewidth may be appreciable in germanium because of the large g anisotropy $g_{\parallel}-g_{\perp}$.

IV. EXPERIMENTAL DETAILS

A. Equipment and Samples

The experiments were performed at ~9000 Mc/sec using a superheterodyne spectrometer which has been described elsewhere.[6] Because of the small binding energy of the donor states, all of the work was done at liquid helium temperatures. The magnetic field was modulated at 100 cps and the bridge tuned to the absorption signal. The relaxation times were short enough that all observations were made under almost slow passage conditions.

The modulation amplitude was usually of the order of 5 Oe and the microwave power to the cavity was of the order of 10^{-5} W to prevent saturation of the signal. The procedure was to sweep the entire spectrum slowly from low to high field and then with reversed direction. The position of the line was based on the average of these two. Field markers were obtained from a proton nuclear resonance probe.

The resonant spectrometer cavity (operating in the Te_{101} mode) was a split pair of silvered glass halves with inside dimension slightly smaller than the sample length so that external stress could be applied to the sample. The loading stress was developed by a calibrated spring and transmitted by a wire and lever system described previously.[8] In most of the work described here, the stress was applied in a direction perpendicular to the direction of the magnetic field.

The magnitude of the stress was determined from the measured spring tension and the known mechanical advantage of the spring squeezing system. The errors in this measurement were of the order of 3%. In estimating the strain in the sample one must also take into account any gradients in strain. These were determined in our experiments by displacing the field slightly from the [100] axis and measuring the increase in linewidth, of the germanium samples. As we have pointed out, a nonuniform strain will produce a distribution of g values and increase the linewidth. The large g shifts in germanium produce a large effect for relatively small deviations from uniform strain. Most of our measurements entailed strain gradients of the order of 5%.

The samples were cut from Czochralski-grown crystals of suitable doping to a size of 1×9×2.2 mm and etched.[27] The etching reduces the possibility of fracture precipitated by surface damage. The samples are oriented within 20 sec by x-ray techniques. The usual orientation of stress applied the external force along a [110] axis of the crystal while the magnetic field was rotated in the (110) plane at right angles. The elastic constant c_{44} for germanium was extrapolated

[27] The samples were etched for 1 min in 5 parts HNO_3 and 1 part HF.

to 1.2°K from the low-temperature measurements of McSkimmin[28] giving $c_{44}=7.00\times10^5$ kg/cm^2.

The resistivity of the samples was measured by passing a current through the long dimension of the sample and measuring the voltage drop across two probes spaced 0.050 in. apart placed at the middle of the sample. The impurity concentrations were then estimated from the measured resistivity and the electron drift mobility values obtained by Prince.[29]

B. Measurements

The determination of the hyperfine splittings and g shifts in germanium requires some care in analyzing because the large linewidths and small spacings cause the lines to overlap. The analysis was based on the assumption that the overlapping lines were always Gaussian in shape. Under very large stresses this is observably not the case; however, for relatively small stresses and small angular shifts from the [100] axis, the results can be reasonably fitted. The problem is most severe for the case of phosphorus-doped germanium and limits the determination of hyperfine splitting to about 5% error. The hyperfine splitting for arsenic can be measured within 3% and that for bismuth within 1%. The accuracy in determining the hyperfine splitting under strain is slightly poorer because the line broadening effects we have mentioned increase the smearing out of the hyperfine spectra. This leads to an over-all error in determining E_{13}/Ξ_μ of 8% for phosphorus donors, and 6% for both arsenic and bismuth donors. The single valley g values for arsenic and phosphorus donors were determined with 6% error. In the case of arsenic and bismuth donors, only the shifts of the $m_D=\pm\frac{1}{2}$ lines were measured. Quadrupole interactions with electric-field gradients introduced under stress will contribute to shift of the other hyperfine lines.[30] We experimentally observe a greater broadening of these lines in stressed samples than of the $m_D=\pm\frac{1}{2}$ lines, as a result of the quadrupole interactions. No attempt has been made to study these effects since they are difficult to separate from those already mentioned.

V. EXPERIMENTAL RESULTS ON UNSTRESSED SAMPLES

A. Donor Ground State

1. Hyperfine Spectrum

The spin resonance spectra for 5×10^{15}/cm^3 arsenic ($I=\frac{3}{2}$) and 8×10^{14}/cm^3 phosphorus ($I=\frac{1}{2}$) donors in germanium at 1.2°K are shown in Fig. 2. These spectra were taken with the magnetic field along the [100] crystal axes and, therefore, correspond to the minimum linewidth condition. A similar spectrum of 10 widely spaced lines was obtained from a sample doped with 3×10^{15}/cm^3 bismuth ($I=\frac{9}{2}$) donors. These experimental results show definitely that the ground state for these three donors in germanium is the singlet. The result for antimony donors in germanium is uncertain since no such hyperfine spectrum was observed in antimony-doped samples of germanium.

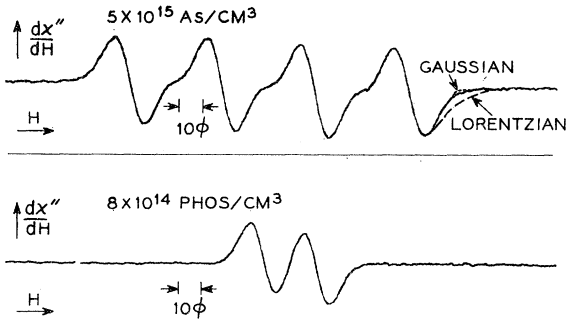

FIG. 2. Electron spin resonance spectrum for arsenic and phosphorus donors in germanium $T=1.2$°K, $H\approx4000$ Oe. Magnetic field along the [100] crystal axis.

The amplitude of the signal, assuming that all donor electrons were in the singlet state, was in good agreement with that of a phosphorus-doped silicon sample with known number of spins. The amplitude of the signal was found to decrease as the temperature was increased in further support of the observation that the spectrum corresponds to the ground state. The experimental results for the observed hyperfine splittings in As-Ge, P-Ge, Bi-Ge, the magnitude of $|\psi_{(0)}|^2$ deduced using the expression [Eq. (8)] and g values are summarized in Table I and compared with similar results for silicon.[6]

Although the magnitude of the hyperfine splitting for arsenic and phosphorus is only slightly smaller in germanium that that in silicon, one might have expected it to be much smaller since the envelope function spreads out much further. However, the hyperfine splitting, as pointed out, also depends on the bunching of the conduction-band wave functions at the lattice centers (η_{Ge}).

2. Estimate of η_{Ge}

Values for η in silicon have been obtained by Shulman and Wyluda[31] and by Solomon[32] from the nuclear spin-lattice relaxation times of Si^{29}. An expression for the spin-lattice relaxation time, T_1, has been given by Abragam[33] in the form

$$\frac{1}{T_1}=\frac{128}{9}(2\pi)^{1/2}\left(\frac{\beta^2\mu_I{}^2}{\hbar^4I^2}\right)\eta^2Nl(m_{\parallel}m_{\perp}{}^2)^{1/2}(KT)^{1/2}, \quad (23)$$

[28] H. McSkimmin, J. Appl. Phys. **24**, 988 (1953).
[29] M. Prince, Phys. Rev. **93**, 1204 (1954).
[30] R. Shulman, B. Wyluda, and P. W. Anderson, Phys. Rev. **107**, 953 (1957).
[31] R. Shulman and B. Wyluda, Phys. Rev. **103**, 1127 (1956). The expression used by Shulman and Wyluda is in error by a factor of 2. However, their mobility data was also in error by roughly the

where N is the density of mobile carriers and l is the number of conduction-band valleys. Wyluda[34] measured the relaxation time for Ge^{73} and found that the relaxation time at 20°K for $N=4\times10^{17}/cm^3$ was approximately equal to that for Si^{29} in silicon samples of impurity concentration $1\times10^{17}/cm^3$ at room temperature. From this result and the expression above we deduce a value for the ratio $\eta_{Ge}/\eta_{Si}=9.5$ and a value for $\eta_{Ge}=1700\pm300$.

Using this result in the expression for the hyperfine splitting (see Sec. IIB) and values for $|F(0)|^2$ obtained from effective-mass theory we obtain estimates for the hyperfine splitting roughly an order of magnitude smaller than those observed. A similar discrepancy occurred in the case of silicon. This discrepancy is attributed to the breakdown of the effective-mass approximation in the near vicinity of the donor impurity.

3. Central Cell Correction

For silicon, Kohn and Luttinger[2] have proposed the following qualitative correction to the effective-mass formalism. Outside the central cell (i.e., $r>r_s$, $4\pi/3r_s^3$ = atomic volume), the effective-mass wave function $F(r)$ is assumed as a solution but with adjusted effective radii (a^*) given by

$$a^*=an=a(E_{\text{eff mass}}/E_{\text{obs}})^{1/2}. \tag{24}$$

This corresponds to a solution of the Schroedinger equation with eigenvalue E_{obs} rather than $E_{\text{eff mass}}$ and since all of the observed ionization energies are lower than the effective-mass value, this solution will go to infinity at the origin. Kohn and Luttinger cut this solution off at the central cell and join it on to an almost atomic wave function. This correction for silicon increases the calculated value of $|F(0)|^2$ for the singlet by almost an order of magnitude, bringing the expected value for $|\psi(0)|^2$ into agreement with experiment.

Kohn and Luttinger have pointed out this correction of the effective-mass formalism essentially holds only for donors with an atomic number close to the host lattice, i.e., phosphorus in Si or arsenic in Ge. The effect of substituting a donor with appreciably larger nuclear change can be seen in the case of bismuth-doped germanium. The $|\psi(0)|^2$ is an order of magnitude larger for bismuth donors than for phosphorus donors.

With respect to this correction, one might have expected the germanium donors to fit the effective-mass approximation somewhat better because of the much larger spread in wave function. The fact that the discrepancy in the vicinity of the impurity in germanium is as large as that in silicon undoubtedly arises from the relatively larger bunching of the germanium conduction-band wave functions at the lattice sites.

TABLE I. g values, linewidth $\Delta H_{Ge^{73}}$ (magnetic-field difference between maximum and minima of the absorption derivative). Total hyperfine splitting and magnitude of the contact term $|\psi_{(0)}|^2$ for donors in germanium and silicon.

Donor	Impurity conc/cm³	g value	Linewidth ΔH (Oe)	Total hfs[a] (Oe)	$\lvert\psi_{(0)}\rvert^2\times10^{24}$ cm^{-3}
		Germanium			
Phosphorus	8×10^{14}	1.5631 ± 0.0002	10 ± 1	21 ± 1	0.17
Arsenic	5×10^{15}	1.5700 ± 0.0002	11 ± 1	107 ± 3	0.69
Bismuth	5×10^{15}	1.5671 ± 0.0004	10 ± 1	944 ± 5	2.15
Antimony	5×10^{15}	1.60 [100]	20 [100]	···	···
		Silicon[b]			
Phosphorus	1.5×10^{16}	1.99850	2.8	42	0.43
Arsenic	1.8×10^{16}	1.99837	3.2	212	1.73
Bismuth	2×10^{16}	2.0003	4.5	···	···
Antimony	2.5×10^{16}	1.99858	2.6	···	1.18

[a] This does not include any Breit-Rabi correction. The g values and $|\psi_{(0)}|^2$ are corrected for the Breit-Rabi effects. [See Appendix G in Ref. 8.]
[b] See Ref. 6.

B. Linewidth in [100] Direction

1. Normal Isotope Samples

As expected, the linewidth in germanium is appreciably larger than in silicon, the ratio of the two being roughly in accord with the ratio of their η's. The linewidth in germanium, however, is very anisotropic with a minimum in the [100] direction. The line broadening effects that set in as the field is rotated will be discussed later; for the moment we will be concerned only with the linewidth for magnetic fields in the [100] direction.

Since the increase in linewidth in germanium over silicon is roughly that expected from its larger η, we conclude that the principal line-broadening effect in the [100] direction arises from the distributed hyperfine interactions with the Ge^{73} nuclei.

2. Isotopically Enriched Sample

Further evidence that the linewidth in the [100] direction arises from the Ge^{73} hyperfine interactions was obtained from the observation of arsenic donor electron spectrum in an isotopically enriched sample that was prepared in the following way.

A single crystal of high-purity germanium was pulled from a melt of isotopically enriched Ge^{74} obtained from the Oak Ridge National Laboratory. The Ge^{73} concentration in this sample was reduced to 0.86%.[35] The crystal preparation has been outlined by Geballe *et al.*[36] Oriented slices from this crystal were subjected to a slow-neutron irradiation which produced $2\times10^{15}/cm^3$

same amount so that their value of $\eta_{Si}=186$ is rather close to the corrected value of $\eta_{Si}=178$ obtained by Solomon (Ref. 32).
[32] I. Solomon (unpublished).
[33] A. Abragam, *Principles of Nuclear Magnetism* (Oxford University Press, New York, 1961).
[34] B. Wyluda, Phys. Chem. Solids **23**, 63 (1962).

[35] The isotopic composition of this sample as compared with normal germanium is

	Ge^{70}	Ge^{72}	Ge^{73}	Ge^{74}	Ge^{75}
Normal germanium	20.45%	27.41%	7.77%	36.58%	7.79%
Enriched germanium	0.80%	1.03%	0.86%	96.75%	0.56%.

[36] T. H. Geballe and G. Hull, Phys. Rev. **110**, 773 (1958).

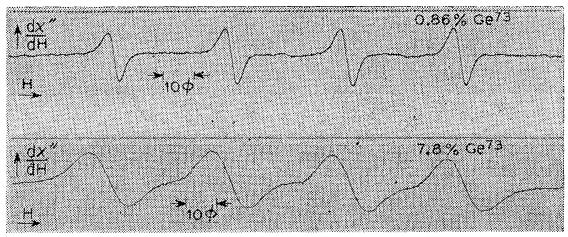

FIG. 3. Comparison of the spectrum for arsenic donors in isotopically enriched germanium, (0.86% Ge^{73}) and normal germanium (7.8% Ge^{73}), $T=1.2°K$, $H=4000$ Oe. Magnetic field along the [100] crystal axis, $N_d \cong 2\times10^{15}/cm^3$.

reactions of the type $Ge^{74}+n=As^{75}$.[37] The sample was annealed at 450°C to relieve radiation damage.[38] As expected, the linewidth for this sample is much reduced (see Fig. 3), the reduction being roughly what one expects on the basis of the linewidth calculation. The calculated ratio of the linewidths for the isotopically enriched sample to one with normal isotopes is $(0.86/7.8)^{1/2}=0.34$, in very good agreement with the observed ratio $3.6/11=0.33$. This result proves that the linewidths in the [100] direction are entirely due to unresolved hyperfine interactions with Ge^{73}. Because of the reduced linewidth and enhanced signal-to-noise ratio, this isotopically enriched sample has proven very useful in other experiments to be described later.

3. *Spread of Wave Function from Linewidth*

From the observed [100] direction linewidths in normal isotope samples and the calculation given in Sec. IIB [Eq. (14)], it is possible to estimate the effective spread of the donor wave function (a_0^*).

There are several sources of error in this calculation that should be noted first. The most significant arising from the assumption of an isotropic envelope function $F(r)$ in obtaining Eq. (14). The actual wave functions are rather pancake-like. Because of the four-valley phase factors, the assumption of an isotropic wave function will particularly alter the contributions from Ge^{73} nuclei on sites along a face diagonal (these will be underestimated). We estimate for the anisotropy (roughly 3:1) predicted by effective-mass theory for germanium that these terms might introduce an error of roughly 30% in the calculation of linewidth. In turn, this would lead to an error of 20% in the estimate of the spread of the wave function.

An additional error occurs because we neglect the build-up of the wave function near the nucleus, which would particularly affect the contribution from the nearest neighbors. However, the phase factors produce a weak contribution from the nearest neighbor term and the effect on the linewidth calculation should be small. This conclusion is supported by the fact that the linewidths (unlike the case in silicon) vary little from donor to donor. That is, the wave function spread is so large that differences of wave function in the vicinity of the central cell have little effect on the linewidth.

From the observed linewidths we obtain the estimated spread in wave function for the three donors given in Table II as compared with values estimated by the corrected effective-mass isotropic approximation. Since we have tended to underestimate the contribution of certain terms in assuming an isotropic wave function, the estimates of wave function spread from the linewidths should be on the low side of the *true* spread.

C. Linewidth Off the [100] Direction

For all of the germanium samples observed, the linewidth was found to increase as the magnetic field moved away from the [100] axis. The broadening was found to vary with the sample and was strongly correlated with the dislocation density. This suggested that the broadening was a result of random g shifts produced by strain associated with the number of dislocations (ϵ). As a check the linewidth off the [100] axis was compared for magnetic fields of 4000 and 10 000 Oe and was found to increase linearly as expected. (Note that this makes very high field spin resonance studies difficult in germanium.) Furthermore, the linewidth in a sample having 2×10^4 ϵ/cm^2 was found to increase drastically when the sample was plastically deformed to introduce 5×10^6 ϵ/cm^2. The variation in linewidth with angle for this sample before and after plastic deformation and several others are shown in Fig. 4. The number of edge dislocations in these samples was determined by counting the density of etch pits produced on a (111) face by a potassium ferrocyanide etch.[39]

At very high dislocation densities, it can be seen that the linewidth increases so rapidly that the lines are

TABLE II. Spread of assumed isotropic effective-mass wave function $F(r)=1/(\pi a_0^{*3})^{1/2}\exp[-(r/a_0^*)]$ for donors in germanium as compared with corrected effective-mass values $a_0^*=(E_{\text{eff mass}}/E_{\text{obs}})^{1/2}(a^2b)^{1/3}$.

Donor	Observed linewidth ($\Delta H_{Ge^{73}}$) (Oe)	Wave-function spread a_0^* from linewidth (Å)	Wave-function spread eff mass calc $n^{1/2}(a^2b)^{1/3}$ (Å)
Phosphorus	10	31.8	38.5
Arsenic	11	29.8	36.8
Bismuth	10	31.8	39.0

[37] In normal germanium, 30% of the captured thermal neutrons give rise to Ga^{71}, 9.8% to As^{75}, and 1.2% to Se^{77}. In the enriched sample, the corresponding reactions are 3.3% to Ga^{71}, 77% to As^{75}, 2.6% to Se^{77}. The remainder of the captured neutrons in both instances give rise to Ge^{73} and Ge^{74}.

[38] The sample irradiation and annealing was generously provided by J. W. Cleland.

[39] The samples are immersed for 5 min in a boiling solution of 8 g $K_3Fe(CN)_6$+12 g KOH in 100 ml H_2O. This etch produces distinctive triangular etch pits corresponding to edge dislocations on (111) faces.

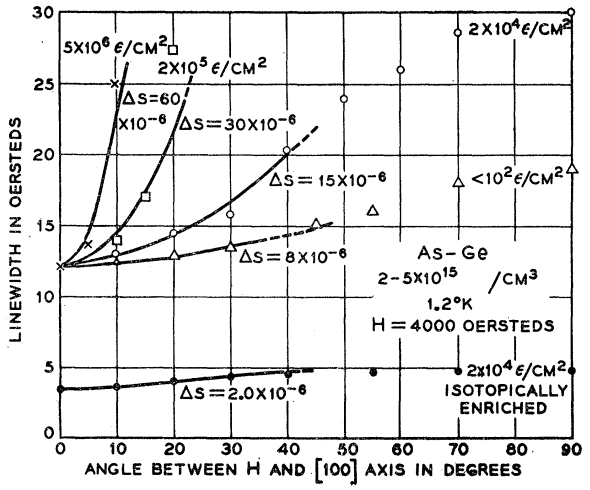

FIG. 4. Linewidth of arsenic-germanium $N_d=2$–$5\times10^{15}/\text{cm}^3$ for magnetic fields off the [100] direction. The various samples have dislocation densities varying from $<10^2$ ϵ/cm^2 to 5×10^6 ϵ/cm^2, and includes the isotopically enriched sample. The solid lines are the theoretical results given by Eq. (22) for various assumed Gaussian average strains (Δs).

washed out a few degrees off the [100] direction. Since the early studies on germanium crystals were probably on rather heavily dislocated material, a slight misorientation of the sample from this axis would have caused the signal to be missed.

In order to compare these results with the calculation in Sec. IIIE, of the line broadening [see Eq. (22)], we have also shown calculated curves (small angles only) for various average Gaussian distributed strains (Δs) assumed to arise from the dislocations.

We find that the broadening for small angles can be fitted by the asumption of a Gaussian average-strain component along the [111] axes. The components along the [110] axes will negligibly contribute for small angles but will add fractionally to the calculated broadening for angles approaching the [110] direction. As expected, the average strain deduced from the line broadening increases with the edge dislocation density. It is important to note, however, that the broadening of the *isotopically enriched sample* is extremely small in comparison with the others in spite of its rather large edge dislocation density ($\sim10^4$ ϵ/cm^2).

In moderately dislocated material the average strain is given by the expression[40]

$$\Delta s\approx10^{-8}(\epsilon/\text{cm}^2)^{1/2}, \qquad (25)$$

For the isotopically enriched sample, this gives an average strain of 1.4×10^{-6}, in good agreement with a value of 2×10^{-6} obtained by fitting the observed broadening. On the other hand, the normal isotope samples show broadenings corresponding to average strains an order of magnitude larger than the above expression yields.

[40] W. T. Read, *Dislocations in Crystals* (McGraw-Hill Book Company, Inc., New York, 1953).

This difference between the isotopically enriched and normal samples arises in the following way: The isotopically enriched sample was doped by neutron irradiation and one can be reasonably certain that the distribution of impurities is random among the dislocations. On the other hand, the normal samples were all doped during the growth process and some degree of association of the donors and the edge dislocations also introduce during growth is not at all unlikely. Hence, the average donor is subject to a strain much larger than that for donors randomly distributed among the dislocations. Our results for donor concentrations of $\sim10^{15}/\text{cm}^3$ imply that most of the donors are trapped in regions relatively near the dislocations rather than distributed in a truly random arrangement.

D. Antimony-Doped Germanium

The experiments with antimony-doped germanium gave various results depending strongly on the sample. In no case was a hyperfine spectrum observed even in lightly-doped samples. Fritzsche has estimated that the singlet-triplet splitting for the antimony donor level is[12] 0.00057 eV so that a strain of only 10^{-5} will produce a significant change in the donor wave function. Such strains are often found in the typical pulled crystal of germanium. As a result, one expects there to be a distribution of hyperfine splittings for the antimony resonance. In view of the fact that there are two isotopes of antimony with spins of $\frac{5}{2}$ and $\frac{7}{2}$, so that a total of 14 lines should appear each with a linewidth of 10 Oe or more, it is understandable that the hyperfine spectrum of antimony has not been observed. An attempt was made to improve the signal-to-noise problem and minimize the effects of intrinsic lattice strain by applying a large static strain in the [111] direction. No resonance in the lightly doped samples was seen under these conditions either.

In more heavily doped samples where motional narrowing occurs, a resonance in antimony-doped germanium was observed with a g_0 in the [100] direction of 1.6. In all such samples except one the line was very broad and became broader as the magnetic field was rotated. In the case of one sample ($N_d=5\times10^{15}/\text{cm}^3$) the line was relatively narrow (20 Oe in [100] direction) and could be observed even in the [110] direction. However, the line was found to shift rapidly with angle, the g in the [110] direction being 1.9. It is possible that a built-in strain existed in this sample causing most of the donor electrons to occupy a single valley. Because of the small singlet-triplet splitting, the strain need not be very large.

Several other considerations made the observation of the resonance in Sb-doped germanium difficult. The relaxation times are expected to be much shorter than for arsenic or phosphorus donors (see Sec. VI). The wave functions are not as compressed so that impurity hopping sets in at lower concentrations. In addition,

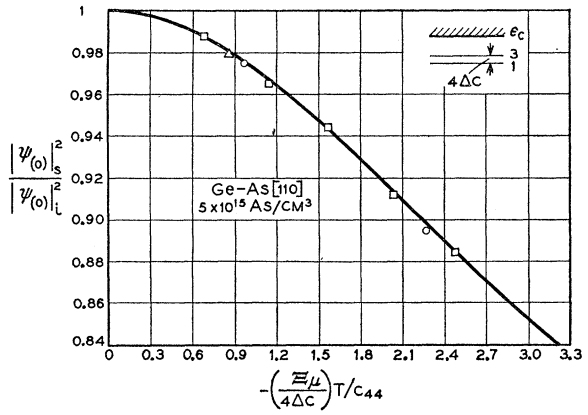

FIG. 5. Ratio of hyperfine splitting with strain to the unstrained value as a function of valley strain $\Xi_\mu s/E_{13}$ for uniaxial compression along the [110] direction. The solid curve represents the fit for Eq. (15) assuming $E_{13}/\Xi_\mu=2.20\times10^{-4}$ eV.

there should be an appreciable lifetime broadening of the triplet states which may be admixed into the ground state to a certain degree by static lattice strains.

Pontinnen and Sanders[41] have observed a spin resonance in antimony-doped germanium having impurity concentrations $>10^{16}/\text{cm}^3$ consisting of four lines having principal g values very near those we have reported. The lines are narrower than those observed for the localized electrons on the other donors, have a much faster relaxation rate, and exhibit a weaker temperature dependence. Their intensities indicate that only 1/40th of the donor electrons are contributing to this resonance. We have examined similar samples but fail to observe the resonances seen by Pontinnen and Sanders. The impurity range covered in Pontinnen and Sanders' samples are in the impurity hopping region so that motionally narrowed lines would be expected in these samples. The narrow lines with short relaxation times observed agree with this conclusion.

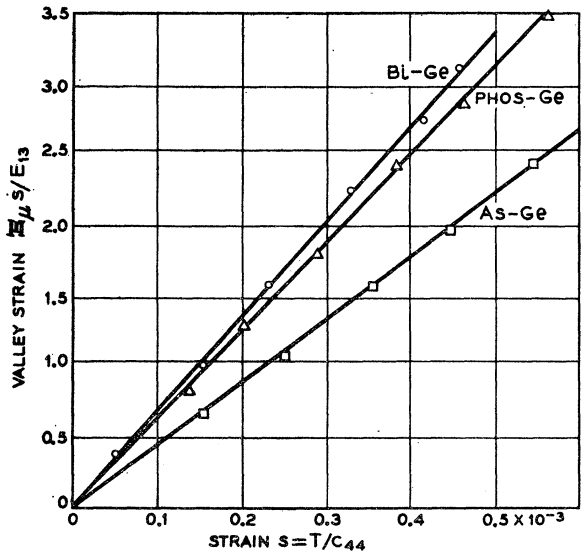

FIG. 6. Valley strain determined by means of Eq. (15) versus elastic strain T/c_{44} for uniaxial compression in the [110] direction, $T=1.2$°K, $\nu=9$ kmc, H parallel to [100]. The lines drawn give the values of E_{13}/Ξ_μ listed in Table III.

VI. EXPERIMENTAL RESULTS ON STRESSED SAMPLES

A. Hyperfine Splitting

The change of the hyperfine splitting under strain discussed in Sec. IIIB, was determined in arsenic-doped germanium for a uniaxial stress in the [110] direction, and the magnetic field along a [100] direction. The results are shown in Fig. 5. These data and similar results on phosphorus- and bismuth-doped germanium have been fitted to the calculated result [Eq. (15)] using the values of E_{13}/Ξ_μ listed in Table III. These results are in good agreement with those of Fritzsche[42] and of Weinreich.[17] Here, as in silicon, there is strong evidence that the change in hyperfine splitting with strain is almost entirely due to the valley repopulating; this is confirmed by the work of Fritzsche.[24] To check this, we have plotted in Fig. 6 the "valley strain" in various samples against the elastic strain where the "valley strain" is estimated from the change in hyperfine splitting. The linear dependence indicates the validity of the assumption made above. The largest strains used here approach 10^{-3} and result in the depressed valleys being occupied 90% of the time. It is quite possible to achieve saturation of the effect at strains approaching 10^{-2}.

TABLE III. Measured values of the ratio E_{13}/Ξ_μ from [110] uniaxial stress for various donors in germanium. Values for the singlet-triplet splitting (E_{13}) are obtained assuming $\Xi_\mu=19$ eV.

Donor	Optical ionization energy[a] (eV)	$E_{13}/\Xi_\mu\times10^4$	E_{13} (eV)	E_3 (eV)
Phosphorus	0.0125	1.53	0.0029	0.0096
Arsenic	0.0145	2.20	0.0042	0.0103
Bismuth	0.0123	1.47	0.0028	0.0095
Antimony	0.0098	···	0.00057[b]	0.0093
Theory	···	···	···	0.0092

[a] See Ref. 44.
[b] See Ref. 12.

The value of Ξ_μ which has been determined experimentally by several workers[42,43] is 19 ± 1 eV at 1.2°K. Using this value and the ratios E_{13}/Ξ_μ we obtain values for the singlet-triplet splitting. Subtracting this from

[41] R. Pontinnen and T. Sanders Jr., Phys. Rev. Letters **5**, 311 (1961).

[42] H. Fritzsche, Phys. Rev. **115**, 336 (1959).
[43] C. Herring and E. Vogt, Phys. Rev. **101**, 944 (1956).

the observed optical ionization energies[44] we can calculate the position of the triplet (E_3). The corresponding levels are shown in Fig. 7. We have also included the value for antimony as determined by Fritzsche.[12] The triplet levels lie very close to that predicted by effective-mass theory (0.0092 eV).

The result that phosphorus and bismuth have the same singlet-triplet splitting is somewhat surprising. That is, we might have expected their respective central cell corrections to be rather different in view of the order of magnitude difference in their $|\psi_{(0)}|^2$.

Under large stresses, the tetrahedral symmetry of the crystal is destroyed and the hyperfine interaction is described by a tensor. The anisotropy in the splitting is small, however, at the level of stress employed here and has been neglected in the calculations.

B. g Shifts Under Strain

As pointed out in Sec. IIIC, the admixing of the triplet into the ground state not only changes the hyperfine interaction but also shifts the center of the resonance spectrum, the magnitude of the shifts depending on the single valley anisotropy term $g_{\parallel}-g_{\perp}$. The g shifts under varying strains were determined as a function of angle θ between the [100] axis and the magnetic field where the stress was applied in a perpendicular [110] direction. Our measurements were restricted to rather small strains and small angles under which case the g shift varies as $\cos^2\theta$. The results are shown for an As-Ge sample in Fig. 8. The observed anisotropies have been fitted to Eq. (19) for both As-Ge and P-Ge and yield the values of g_0, $g_{\parallel}$, and $g_{\perp}$ listed in Table IV.

TABLE IV. Values for single-valley g's in arsenic- and phosphorus-doped germanium as compared with the theory of L. Roth.[a] These values were obtained from g shifts of respective spectra under [110] uniaxial compression.

Donor	g_0	$g_{\parallel}-g_{\perp}$	$2-g_{\parallel}$	$2-g_{\perp}$
Arsenic	1.570	-1.05 ± 0.06	1.13 ± 0.04	0.08 ± 0.02
Phosphorus	1.563	-1.10 ± 0.07	1.17 ± 0.05	0.07 ± 0.02
Theory	1.70	-1.09	1.02	-0.07

[a] See Ref. 10.

Listed also are the theoretical values of Roth.[10] The agreement in the case of $g_{\parallel}$ is rather good, but the value of $g_{\perp}$ deviates from two in the wrong direction. The failure to fit experiment has been examined in more detail by Liu[11] who found the two-band approximation inadequate for silicon. In the case of germanium, he finds it should be essentially correct but finds no reason for the discrepancy between theory and experiment. The small shift of the $g_{\perp}$ from two does suggest, as was the case for silicon, that contributions to the g shift from bands other than the valence band may also be important.

[44] H. Y. Fan and P. Fisher, Phys. Chem. Solids 8, 270 (1962).

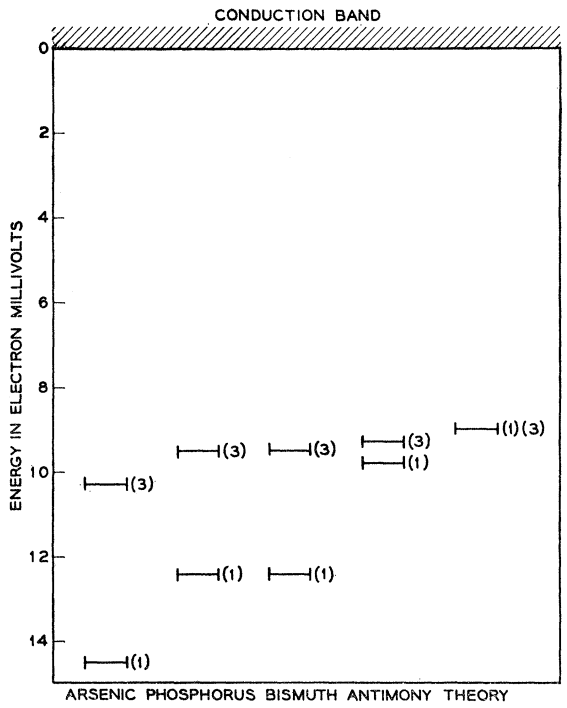

FIG. 7. Energy level scheme for donor electrons in phosphorus-, arsenic-, bismuth-, and antimony-doped germanium (assuming $E_{\mu}=19$ eV) as compared with the effective-mass theoretical value.

In the case of silicon, the application of uniaxial stress along the [111] axis produced a g shift by altering the single-valley anisotropy.[8] A similar effect in germanium would lead to a g shift for uniaxial stress in the [100] direction. The presence of such an effect would yield wrong experimental values for $g_{\parallel}$ and $g_{\perp}$ for a [110] uniaxial compression. As a check, we looked for a g shift in As-Ge with uniaxial stress applied in the [100] direction. No shift was observed within the accuracy of our measurements. Because of the gradient in strain, this

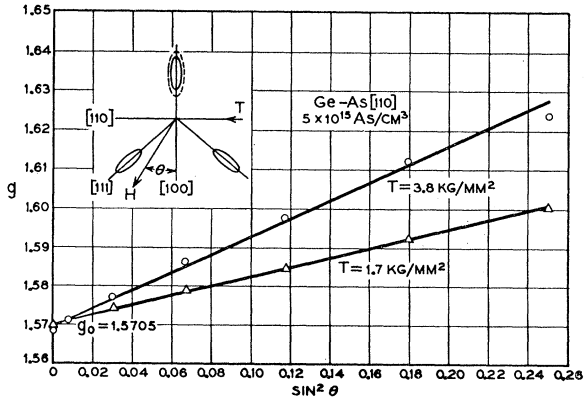

FIG. 8. g shift versus $\sin^2\theta$ for arsenic-germanium. (θ is angle between the [100] axis and the magnetic field) for uniaxial compression in the [100] direction perpendicular to the plane of the magnetic field. Note g shift vanishes in [100] direction.

result is good to about 3%. Nakayama and Hasegawa[45] have estimated the magnitude of the one-valley g shift in germanium to be less than this experimental uncertainty.

C. Linewidths Under Strain

Under large stresses ($x>1$) in [111] direction, the linewidths observed in the [100] direction have been found to decrease as much as 10%. This is somewhat less than expected from the valley repopulating effect (see Sec. IIID). However, strain gradients and misalignment of the sample will tend to reduce the degree of narrowing.

As one moves off the [100] axis, however, the small gradients in the strain cause the linewidths to increase. At large strains where the shift from g_0 approaches 0.5, a strain gradient of 5% would result in a linewidth of the order of 100 Oe at large angles so that the lines are essentially wiped out. Consequently, no studies of the line broadening off the [100] axis in strained samples have been made. As pointed out, however, we have as a matter of record, compared the broadening at small angle to the shift in the center of the line in order to estimate the magnitude of the strain gradient in the sample.

An additional contribution of the linewidth under strain comes from the quadrupole interaction of the Ge^{73} and the crystal fields.[30] The effect is small compared to the others we have considered and has not been studied.

VII. SPIN-LATTICE RELAXATION TIMES

A. Relaxation Mechanisms

When the equilibrium donor electron spin distribution is perturbed as by passage through the resonance, the disturbance decays with a characteristic relaxation time. The most important relaxation processes at helium temperatures in semiconductors have been analyzed by Pines, Bardeen, and Slichter,[46] Abrahams,[47] Roth,[10] and Hasegawa.[13]

At these temperatures the mechanisms which they have shown to be dominant include spin exchange between the donor electrons and conduction electrons (T_c), which can be minimized by using lightly doped samples, relaxation through the modulation of the hyperfine interaction by lattice phonons (T_x), and relaxation through the phonon modulation of the spin-orbit interaction (T_s). In silicon the T_x mechanism has been found to be the dominant one for arsenic- and antimony-doped samples[7] and one might have expected it to be important in germanium as well for the following reason. The magnitude of the relaxation rate $1/T_x$ will depend on the ratio $(\Xi_\mu/E_{13})^2$ for the donor and host involved. If we compare arsenic-doped germanium and silicon we find this mechanism will cause the germanium donor spins to relax two orders of magnitude faster than the silicon donors. In spite of the enhanced relaxation from this mechanism, we will see shortly that relaxation through the third mechanism (T_s) will most certainly dominate the T_x mechanism in any of the germanium samples.

The T_s mechanism has been dealt with in detail by Roth and by Hasegawa. In particular, they have considered a single-phonon process that operates in the following way. The time-varying strain of a lattice vibration with frequency equal to the Larmor frequency produces a time-varying mixture of the triplet and singlet states. Because of the different g values of the singlet and triplet, the electron spin sees a time-varying effective magnetic field at the Larmor frequency which can relax the excited spins. For this one-phonon process, Roth and Hasegawa find that the relaxation rate takes the following form:

$$\frac{1}{T_s}=\frac{4}{\pi}\left(\frac{g_{\parallel}-g_{\perp}}{g_0}\right)^2\left(\frac{\Xi_\mu}{E_{13}}\right)^2\left(\frac{1}{\rho_0 c^5}\right)\left(\frac{g\beta H}{\hbar}\right)^4 KTf(\theta,\varphi), \quad (26)$$

where ρ_0 is the density of germanium and c a suitable average of its sound velocities. The angular factor $f(\theta,\varphi)$ takes on the following values in germanium for

$$H_{\parallel}[100]f_{Ge}=1\,,\ H_{\parallel}[110]f_{Ge}=\tfrac{1}{2}\,,\ H_{\parallel}[111]f_{Ge}=\tfrac{1}{3}.$$

A similar expression obtained by Roth and Hasegawa for silicon has been found to agree closely with experiment.[8] Since $g_{\parallel}-g_{\perp}$ is three orders of magnitude larger in germanium than in silicon, one expects that the relaxation rate in germanium would be controlled by this mechanism and should be roughly six orders of magnitude greater than in silicon, or roughly 10^3 sec^{-1}.

At elevated temperatures, Roth and Hasegawa suggest that the relaxation should be controlled by inelastic scattering of phonons, that is by a Raman process, the interaction with the spins again occurring through the spin-orbit interaction. Their analysis leads to a temperature dependence of the relaxation rate of T^7 and a field dependence of H^2.

Because of the great difference in relaxation rate expected between germanium and silicon arising from the same mechanism, it was of interest to study the relaxation rate in germanium.

B. Relaxation Time Measurements

The measurements in germanium, however, are not as straightforward as they are in silicon by virtue of the much shorter relaxation time. The poor signal-to-noise ratio precludes adiabatic fast-passage techniques to obtain a dynamic measurement of the relaxation time and one is limited, therefore, to a power saturation measurement.

[45] M. Nakayama and H. Hasegawa, J. Phys. Soc. Japan **18**, 229 (1963).
[46] D. Pines, J. Bardeen, and C. P. Slichter, Phys. Rev. **106**, 489 (1957).
[47] E. Abrahams, Phys. Rev. **107**, 491 (1957).

This type of measurement has been described in detail by Bloembergen, Purcell, and Pound.[48] One measures the signal amplitude of the spectrometer as a function of the microwave magnetic field ($2H_1 \sin\omega t$) in the cavity. As H_1 is increased, the number of stimulated transitions eventually approaches the number of absorptive ones, the amplitude of the absorption signal decreases and the transition is said to saturate. The faster the relaxation rate, the larger must H_1 be to achieve saturation.

The saturation behavior depends on such conditions as the modulation frequency (ω_m), the amplitude of the modulation (H_m), the rate of passage through the resonance, etc., in so complicated a manner that only a few of the many passage conditions have been explicitly analyzed.[49,50] In most of our experiments the relaxation times and modulation frequencies were such that $\omega_m T_s \approx 1$. This is an intermediate case which has not been analyzed. However, it was pointed out by Bloembergen *et al.*, in the case $\omega_m T_s > 1$, the saturation should be expressed in terms of a saturation parameter $s=\gamma H_1^2 T_s/H_m$, where γ is the gyromagnetic ratio. The modulation amplitude H_m appears in this expression because the microwave power is essentially spread over the modulated region. Experimentally, we have verified the functional dependence of the saturation in our samples on the ratio H_1^2/H_m.

Further evidence that the case $\omega_m T_s \approx 1$ holds for our samples (for modulation frequencies of 100 or 1000 cps) is obtained from the behavior of the dispersion derivative signal as the modulation amplitude is increased. Increasing H_m should reduce the saturation. As pointed out by Halbach[51] in the range $\omega_m T_s \approx 1$, this leads to a shift in the phase and ultimately to inversion of the dispersion signal. This behavior is verified by the marked changes in the line shape shown in Fig. 9. As we will point out later, this behavior can be used to detect small differences in the degree of saturation.

For the usual power saturation measurement the degree of saturation can be expressed as the ratio (B) of the saturated absorption derivative signal produced by a lock-in detector (proportional to the in-phase component at the modulation frequency) to the signal produced with vanishingly small saturation. This ratio of the absorption derivatives for the case where $\omega_m T_s > 1$ is given by Portis[50] as

$$B=(1+s)^{-1/2}. \tag{27}$$

This expression has been found to fit the observed data rather well over a wide range of relaxation times and passage conditions, although for some of the conditions where ($\omega_m T_s \lesssim 1$) a steeper dependence might have been expected. Because of this ambiguity in the interpretation of the saturation data, we have attempted to bridge the range of experimental conditions by determining the relaxation time from the condition $s=1$ when $B=0.5$. Since the various passage conditions might cause B to be between 0.3–0.7 when $s=1$, we expect the relaxation time estimates to be accurate within 40%.

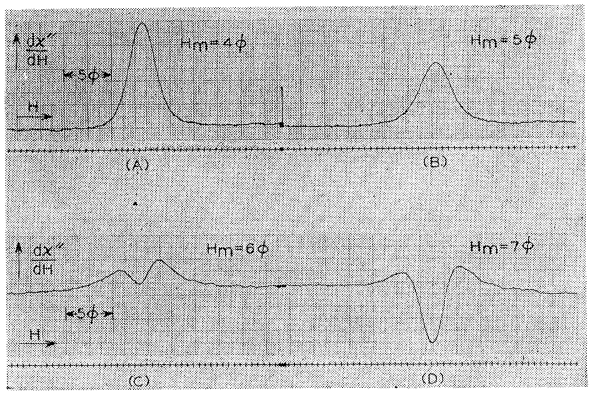

FIG. 9. Relative amplitude of the in-phase dispersion derivative versus magnetic field for increasing modulation amplitude (decreasing saturation) in isotopically enriched arsenic-germanium. The behavior of the dispersion signal indicates that the spin system is not able to recover completely between successive passages of the magnetic field.

C. Experimental Method

To improve the signal-to-noise ratio, most of the measurements of relaxation times were made on the arsenic-doped isotopically enriched sample that was previously described. The doping level of $2\times10^{15}/\text{cm}^3$ was low enough to prohibit relaxation by impurity conduction mechanisms (see Sec. VIIIB). The reduced linewidth permitted observations over a wide range of experimental conditions and inhibited spin transfer which might occur between the overlapping lines found in normal samples. Finally, the increase in linewidth for H not along the [100] axis was small enough that it was possible to study the anisotropic effects.

Since this sample has small amounts of compensation and unannealed radiation damage produced during neutron irradiation, its saturation behavior was compared with that of a normal isotope sample of similar doping at 1.2°K with H along [100]. The saturation behavior of the two was the same within the accuracy of the measurements.

The average saturation behavior of all four lines was observed using 100-cps modulation of 5 Oe so as to saturate all of the line simultaneously and eliminate spin diffusion processes within one hyperfine line. The 100-cps modulation was used in preference to higher modulation frequencies because it was impossible at high-modulation frequencies to prevent signal distortion from small admixtures of the much stronger dispersion signal at high saturation levels.

[48] N. Bloembergen, E. M. Purcell, and R. V. Pound, Phys. Rev. **73**, 679 (1948).
[49] M. Weger, Bell System Tech. J. **34**, 1013 (1960).
[50] A. Portis, Sarah Mellon Scaife Radiation Laboratory, University of Pittsburgh, Pittsburgh, Pennsylvania, 1955, Technical Note No. 1 (unpublished).
[51] K. Halbach, Helv. Phys. Acta **27**, 259 (1954).

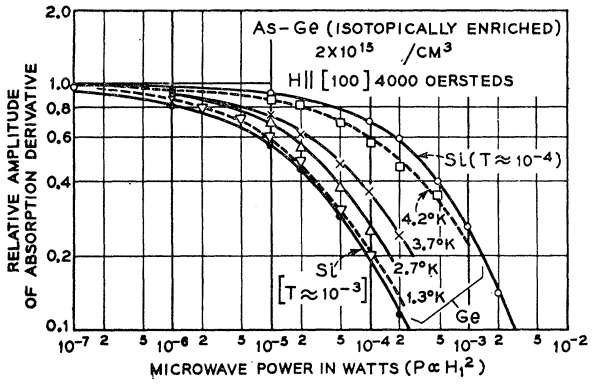

FIG. 10. Saturation behavior of isotopically enriched arsenic-germanium at various temperatures. The solid lines show similar behavior for phosphorus-doped silicon ($N_d=2\times10^{17}/\text{cm}^3$, $T_s\sim10^{-3}$ sec and $N_d=3\times10^{17}$, $T_s\sim10^{-4}$ sec).

The microwave field in oersteds in the cavity was obtained from the microwave power P (in watts) entering the cavity and from the measured Q, using the expression

$$H_1^2=(32\pi Q/\omega V)[1-R^2]P, \tag{28}$$

where V is the volume of the cavity in cm³ and where the coupling was adjusted to give a reflection coefficient $R=\frac{1}{2}$. The measured Q of the X-band cavity was 6000 and that of the K-band cavity was 2000. The H_1 obtained from this expression is the value at the center of the sample. Because a sample of the full width of the cavity was required, the microwave field varies across the sample so that the degree of saturation is not uniform. We estimate the error in determining H_1 from this effect and from the Q measurement is about 30%.

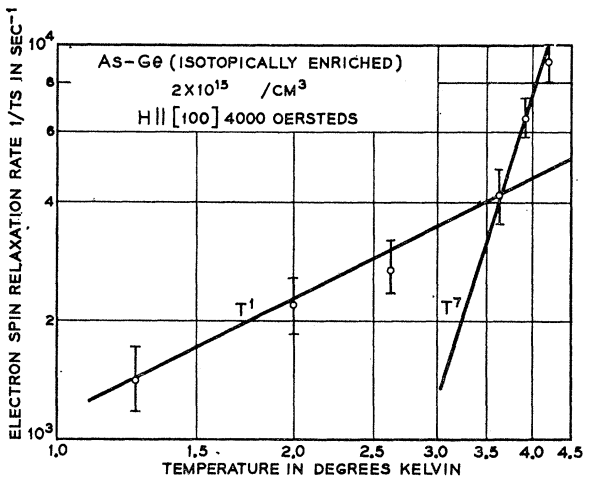

FIG. 11. Relaxation rates estimated from saturation behavior of isotopically enriched arsenic-germanium of Fig. 10 by assuming ($\gamma H_1^2T_s/H_m=1$) when relative amplitude of absorption derivative falls to $\frac{1}{2}$. Below 3.6°K the rate increases linearly with T indicating a single-phonon process.

D. Experimental Results

The saturation behavior for the isotropically enriched sample for temperatures from 1.2 to 4.2°K for H along [100] is shown in Fig. 10. For comparison, we have also shown the saturation behavior for two phosphorus-silicon samples ($H_m=2$ Oe) whose relaxation times were estimated from their impurity concentrations ($3\times10^{17}/\text{cm}^3$, $T_s\sim10^{-4}$ sec, $2\times10^{17}/\text{cm}^3$, $T_s\sim10^{-3}$ sec), and from results of Feher and Gere.[7] The relaxation rates estimated by the procedure given above for the germanium sample are shown in Fig. 11 as a function of temperature. The value obtained at 1.2°K, $1/T_s=1.2\pm0.6\times10^3$ sec^{-1} is in very good agreement with that calculated by Hasegawa ($1/T_s=2\times10^3$ sec^{-1}). Below 3.5°K the rate is found to increase linearly with temperature in agreement with a single-phonon process. Above 3.5°K the rate increases much more rapidly similar to the effect in silicon which has been ascribed to a Raman-type process.

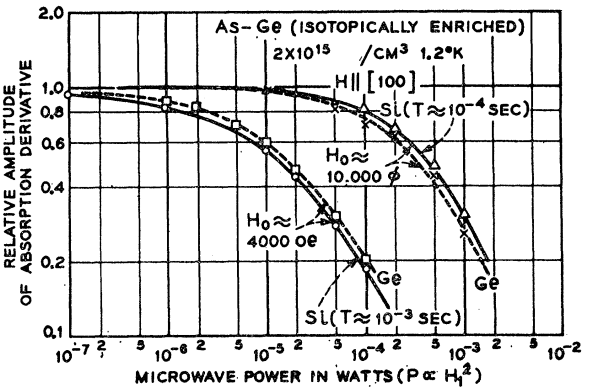

FIG. 12. Change in saturation behavior of isotopically enriched arsenic-germanium with magnetic field. The increase in relaxation rate by more than an order of magnitude also agrees with expected magnetic field dependence of a single-phonon process (H^4).

The saturation behavior for this sample was also measured at K band ($H=11\,000$ Oe) at 1.2°K and the results are shown in Fig. 12, again as compared with a silicon sample ($3\times10^{17}/\text{cm}^3$) also measured at K band. The estimated relaxation rate is $1/T_s=4\pm2\times10^4$ sec^{-1} for H along [100]. This result is consistent with the H^4 dependence for the single-phonon process.

Although the results are in good agreement with the Roth-Hasegawa theory, they do not preclude the possibility that some other single-phonon process may be present. To eliminate that possibility, it was desirable to check the angular dependence of the relaxation rate. For the orientation of this sample it was only possible to rotate the magnetic field in a (100) plane for which the maximum change in the relaxation rate expected was a factor of two. The saturation behavior for the [110] and [100] directions are compared in Fig. 13. The change in the relaxation rate is approximately $\frac{1}{2}$ as predicted by the Roth-Hasegawa theory.

In view of the small changes in saturation, a more sensitive test for changes in the relaxation rate based on a method suggested by Hyde[52] also was used. The microwave field was held constant and the saturation condition changed by changing the modulation amplitude. The degree of saturation was measured by the changes in the line shape of the dispersion derivative (as in Fig. 9). The modulation amplitude was then set to produce a line shape as in Fig. 9(c). We found this method quite sensitive to small changes in the relaxation rate.

The relative modulation amplitude as a function of the angle between H and the [100] axis is shown in Fig. 14. The agreement is quite good with the expected dependence of the Roth-Hasegawa theory. Since the modulation amplitude which yielded the line shape in Fig. 9(c) was always greater than the linewidth (see Fig. 8), the changes in linewidth with angle should have no effect.

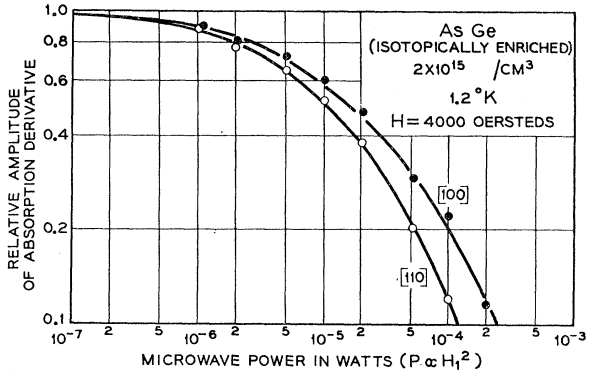

FIG. 13. Change in saturation behavior of isotopically enriched arsenic-germanium as magnetic field is rotated with respect to crystal axes. The decrease in the relaxation rate as H moves from [100] to [110] is approximately $\frac{1}{2}$ in agreement with Roth-Hasegawa theory.

A further test of the Roth-Hasegawa theory can be made by measuring the change in saturation behavior for a sample under uniaxial stress. Such stress not only favorably populates certain of the valleys but also moves the nearest levels further away in energy. This can be seen in Fig. 1. Since the relaxation rate depends quadratically on this energy separation, it should be possible to appreciably reduce the relaxation rate by applying large stresses to the sample. The largest effects should be expected for a stress in the [111] direction in phosphorus-doped germanium. Because of the distortion of the line shape under the large stresses involved, it is difficult to interpret the results directly in terms of relaxation times. The change in the saturation behavior for such a stressed sample for H in the [100] direction at $H=4000$ Oe and at 1.2°K are shown in Fig. 15 with modulation of 10 Oe.

[52] J. Hyde, Phys. Rev. **119**, 1483 (1960).

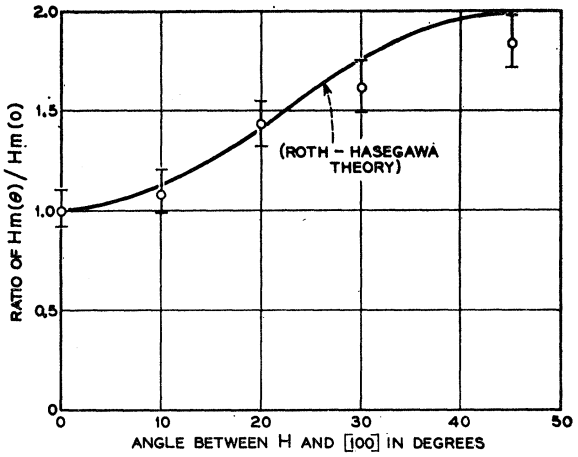

FIG. 14. Modulation field H_m which produces an in-phase dispersion derivative signal shape as in Fig. 9(c) as a function of angle between H and the [100] axis. The solid line is the relative amplitude expected by Roth-Hasegawa theory assuming that the saturation parameter $s=(\gamma H_1^2 T_s/H_m)$.

At large stresses, the decrease in saturation power is in good agreement with the expected increase in the relaxation time by an order of magnitude.[53]

The sum of evidence then strongly supports the Roth-Hasegawa mechanism for spin-lattice relaxation at liquid helium temperatures in germanium as well as in silicon. In view of the fact that the relaxation times of these two materials span six orders of magnitude, the theoretical fit is rather remarkable.

At large [111] stresses which populate a single valley, it should be possible to reduce the relaxation rate appreciably. As we have pointed out, one should also obtain a narrower line under such conditions as well as eliminate the effects of random lattice strains. Under such circumstances it may be possible to study many other effects in germanium that are presently not pos-

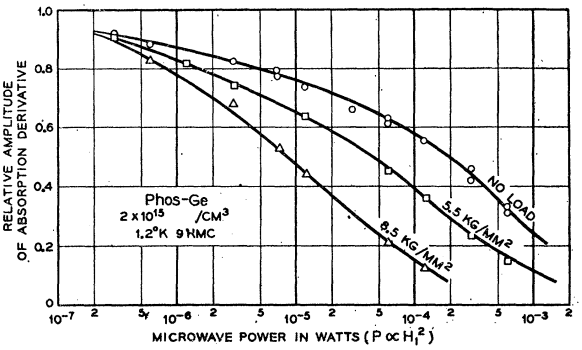

FIG. 15. Change in saturation behavior of phosphorus donors in germanium due to uniaxial stress in the [111] direction. Magnetic field along [100]. The decrease in relaxation rate is roughly that expected from increased splitting of singlet and triplet states.

[53] This calculation is given in detail by Nakayama and Hasegawa (Ref. 45). These authors also have considered other effects of strain on spin resonance of donors in silicon and germanium.

sible because of the rapid relaxation, the linewidth, or the effects of random strains.

VIII. NONLOCALIZED ELECTRONS

A. Effect of Hopping on Resonance Spectrum

As the concentration of donors is increased, the donor wave functions begin to overlap. If compensating impurities are present so that some electrons are removed from the donor sites, there will be a finite probability that an electron on one donor may hop to a nearby unoccupied donor. The electrons can no longer be considered localized on a given donor site. This process is characterized by some average hopping frequency. The hopping rate (u) for lightly doped material has been calculated by Miller and Abrahams[14] and their result for an isotropic wave function is

$$u=\left(\frac{e}{\hbar}\right)^4\left(\frac{\Xi_\mu}{3K}\right)^2\frac{1}{\rho_0 c^5}\left(\frac{R_s}{a^*}\right)^{3/2}\times\exp\left(-\frac{2R_s}{a^*}\right)\Delta\coth\left(\frac{\Delta}{2KT}+1\right), \quad (29)$$

where Δ is the activation energy for hopping and R_s is the average distance between donors ($R_s=0.62N_d^{1/3}$).

At low hopping rates the spin-resonance spectrum will be unaffected, but as the concentration is increased so that the hopping rate begins to approach a frequency corresponding to the donor hyperfine splitting, this splitting tends to be averaged out and a large line appears roughly at the center of the hyperfine spectrum. Further increases in concentration cause this line to decrease in width and increase in amplitude until it is the only line observed.

At 1.2°K the broad background line which indicates the onset of hopping sets in at concentrations of about $10^{15}/\text{cm}^3$ in phosphorus-doped germanium and about $5\times10^{15}/\text{cm}^3$ in arsenic-doped germanium. These values compare well with estimates for the onset of impurity conduction.[16] The difference between phosphorus and arsenic-doped samples can be attributed to differences in the spread of the donor wave functions.

The effect of the motional narrowing on the hyperfine split lines has been analyzed by Weiss and Anderson[54] and they find for the linewidth of the narrowed line

$$\Delta H=g\beta\Delta H_{\text{hfs}}^2/\nu, \quad (30)$$

where ΔH_{hfs} is the magnitude of the hyperfine splitting and ν is the average hopping frequency. Combining this result with that of Abraham and Miller, we expect the linewidth to increase exponentially with the average distance between donors at a rate determined by the spread of the wave function (a). [Note that the overlap of the wave functions depends on the lateral spread of the pancake-like wave functions a rather than on the average spread $a_0^*=n(a^2b)^{1/3}$.]

[54] P. W. Anderson and P. R. Weiss, Rev. Mod. Phys. **25**, 269 (1953).

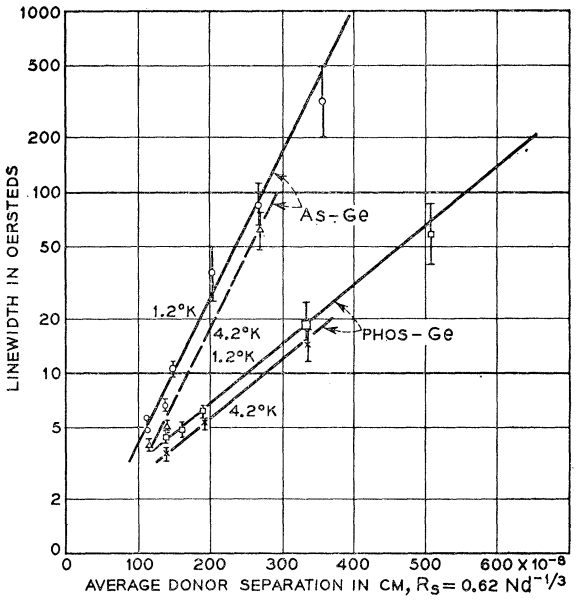

FIG. 16. Linewidth of motionally narrowed line for nonlocalized donor electrons for arsenic and phosphorus-doped gemanium as a function of the "average" donor separation (R_s) rdefined by $R_s=0.62N_d^{-1/3}$ where N_d is the donor concentration. The slopes of the lines give average wave function spreads [$a_0^*=na^*$] of 100 Å for As-Ge and 260 Å for P-Ge.

B. Experimental Results

1. Linewidth in [100] Direction

In Fig. 16 we show the dependence of the motionally narrowed linewidth on the average donor separation for arsenic and phosphorus donors at 1.2 and 4.2°K. The slope of the arsenic line corresponds to a donor wave function spread of 100 Å as compared with the effective-mass estimate of 60 Å; the phosphorus slope, on the other hand, gives donor wave function spread of 260 Å as compared with the effective-mass estimate of 70 Å.

In view of the fact that the linewidths in the [100] compared rather well with the effective-mass estimates for the average speed of the wave function, we believe the above results are due to closer spacing of the donors than a purely random arrangement allows. This could, of course, be the result of clustering of the donors about dislocations as we have already suggested. Our results here, furthermore, indicate that the effect is much more pronounced in the case of phosphorus donors than for arsenic donors.

The activation energies (Δ) which appear in the Miller and Abrahams expression can be found from the change in linewidth with temperature. From the results shown in Fig. 15 we estimate the activation energies to be 0.00035 eV for arsenic donors and 0.00055 eV for phosphorus donors.

The g values for the motionally narrowed lines at

donor concentrations up to $10^{17}/cm^3$ do not shift measurably from their respective localized donor values. Were the electrons free most of the time we would have expected the *same g* value for all donors. We conclude then that the electrons still spend most of the time localized at donor sites at concentrations up to $10^{17}/cm^3$.

As the donor concentration is increased, the onset of hopping will also increase the rate with which the donor-electron spins relax through spin exchange with the nonlocalized electrons. In arsenic-doped germanium with $10^{17}/cm^3$, the relaxation rate at 1.2°K increased to 10^5 sec^{-1} or roughly two orders of magnitude over the nonlocalized value.

2. *Linewidth off [100]*

Since the strain gradients that give rise to the broadening of the hyperfine lines as the magnetic field is rotated away from the [100] direction exist over regions that are large compared to the hopping distances, the line broadening due to strains will not be averaged out by motional narrowing. However, because the hyperfine structure is wiped out, the smear of close-spaced broad lines of the localized electron case is replaced by a single broad line at the center of the spectrum. Figure 17 shows this motionally narrowed line for H in the [100] and [110] directions. The line shape in the [100] is Lorentzian as expected for a motionally narrowed line. However, it is more nearly Gaussian in the [110], a result that can be fitted by assuming a Gaussian distribution of strains in the sample. The linewidth in this case can again be calculated from the expression [Eq. (22)] except that the motionally narrowed width in the [100] replaces that due to the Ge^{73} hyperfine interactions. The linewidths observed off the [100] are again strongly correlated with edge dislocation densities of the samples. For example, the linewidths in Fig. 17 are for a sample of 2×10^4 edge-dislocations/cm^2. The linewidth for a sample of the same impurity concentration but having only 10 edge-dislocations/cm^2 had a linewidth half as large in the [111] direction. This result and the fact that the linewidths are greater than anticipated indicates that the clustering of donors near dislocations which was discussed in Sec. VD is still evident at donor concentrations up to $10^{17}/cm^3$.

C. Effect of Strain

The linewidth of the motionally narrowed line in the [100] direction is very sensitive to uniaxial strain since it is thereby possible to change the wave function overlap and hence, the hopping rate. For example, it was found possible to reduce the linewidth in $5\times10^{16}/cm^3$ phosphorus-doped germanium by a factor of four with a uniaxial stress of 6 kg/mm^2 along [111]. This effect as pointed out by Fritzsche[55] agrees with the observed changes in impurity conduction under [111] uniaxial compression. Since the variation in hopping frequency should be calculable from the observed linewidths, this method may be of some value in studying the impurity conduction mechanism at low concentrations.

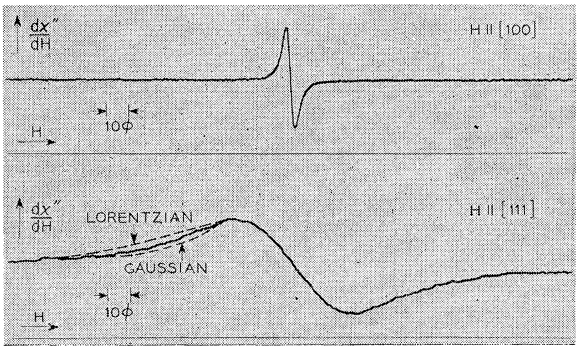

FIG. 17. Spin resonance spectrum for arsenic donors in germanium, $N_d=6\times10^{16}/cm^3$ showing the motionally narrowed line shapes for magnetic field along [100] and [111] directions. $T=1.2$°K, $H\sim4000$ Oe. The line shape in [100] direction is very nearly Lorentzian while that in the [111] direction is more nearly Gaussian. This sample had a dislocation density $=2\times10^4$ ϵ/cm^2.

ACKNOWLEDGMENTS

For the over-all direction and supervision of this work I am especially indebted to G. Feher. I am also indebted to E. Abraham, Y. Yafet, H. Hasegawa, and W. Kohn for their many suggestions. I would also like to thank E. Gere for his help with the experiments, and J. W. Cleland for the neutron irradiation of the isotopically enriched sample.

APPENDIX A: VALLEY POPULATIONS UNDER STRAIN

1. [110] Compression

The strain components for a uniaxial stress T applied to the [110] axis are given by

$$u_{ij}=\begin{vmatrix} S_{11} & S_{12} & S_{12} & 0 & 0 & 0 \\ S_{12} & S_{11} & S_{12} & 0 & 0 & 0 \\ S_{12} & S_{12} & S_{11} & 0 & 0 & 0 \\ 0 & 0 & 0 & S_{44/2} & 0 & 0 \\ 0 & 0 & 0 & 0 & S_{44/2} & 0 \\ 0 & 0 & 0 & 0 & 0 & S_{44/2} \end{vmatrix} \cdot \begin{vmatrix} 1 \\ 1 \\ 0 \\ 1 \\ 1 \\ 0 \end{vmatrix} \cdot \frac{T}{2}. \quad \text{(A1)}$$

Using Herring s notation for the deformation potential

$$E^{\alpha}=[\Xi_d\delta_{ij}+\Xi_\mu K_i^{(\alpha)}K_j^{(\alpha)}]u_{ij}, \quad \text{(A2)}$$

where Ξ_μ is the deformation potential for shear and Ξ_d for dilation, $\mathbf{K}^{(i)}$ is unit vector to the ith valley. We find, then, for the energy shifts with respect to the energy center of gravity, $E_{c.g.}$,

$$\begin{aligned} E^{1,2}-E_{c.g.}&=\Xi_\mu T/6c_{44}, \\ E^{3,4}-E_{c.g.}&=-\Xi_\mu T/6c_{44}. \end{aligned} \quad \text{(A3)}$$

[55] H. Fritzsche, Phys. Rev. **125**, 1552 (1962).

The unstrained valley-orbit matrix is given by

$$-H_{\rm vo}=\begin{vmatrix}0&\Delta_c&\Delta_c&\Delta_c\\ \Delta_c&0&\Delta_c&\Delta_c\\ \Delta_c&\Delta_c&0&\Delta_c\\ \Delta_c&\Delta_c&\Delta_c&0\end{vmatrix}. \tag{A4}$$

Substituting into this Hamiltonian term, the effect of a [110] stress gives the strained valley-orbit term

$$-H_{\rm vo}{}^s=\Delta_c\begin{vmatrix}-\frac{2}{3}x&1&1&1\\ 1&-\frac{2}{3}x&1&1\\ 1&1&+\frac{2}{3}x&1\\ 1&1&1&+\frac{2}{3}x\end{vmatrix},$$

$$x=\Xi_\mu T/4\Delta_c c_{44}. \tag{A5}$$

Generalizing the valley populations [Eqs. (A3,4)] for a [110] stress, we solve the Hamiltonian for a wave function with valley populations $[\alpha_1\alpha_1\alpha_2\alpha_2]$ and find

$$E/\Delta_c=[1-\tfrac{2}{3}x]+2\alpha_2/\alpha_1=[1+\tfrac{2}{3}x]+2\alpha_1/\alpha_2. \tag{A6}$$

Using the normalization condition

$$\sum_{j=1}\alpha_j{}^2=1, \tag{A7}$$

we find

$$\alpha_1{}^2=\tfrac{1}{4}[1-(x/3)(1+x^2/9)^{-1/2}],$$
$$\alpha_2{}^2=\tfrac{1}{4}[1+(x/3)(1+x^2/9)^{-1/2}]. \tag{A8}$$

This gives for the energy shifts under a [110] uniaxial compression

$$E^{a,b}/\Delta_c=-1\pm2(1+x^2/9)^{1/2} \tag{A9}$$

for the ground state and one of the triplet states and

$$E^{c,d}/\Delta_c=1\pm\tfrac{2}{3}x \tag{A10}$$

for the triplet states described by valley populations $(0, 0, \alpha, -\alpha)$. These are the results plotted in Fig. 1.

For the ratio of hyperfine splitting in strained to unstrained sample, we obtain

$$\frac{|\psi_{(0)}|_s{}^2}{|\psi_{(0)}|_i{}^2}=\tfrac{1}{4}[\sum_1^4\alpha_j]^2$$
$$=\tfrac{1}{2}[1+(1+x^2/9)^{1/2}]. \tag{A11}$$

2. [111] Compression

$$u_{ij}=|S_{ij}|\cdot\begin{vmatrix}1\\1\\1\\1\\1\\1\end{vmatrix}(T/3) \tag{A12}$$

and the shifts from $E_{\rm c.g.}$ are

$$E^1-E_{\rm c.g.}=\Xi_\mu T/3c_{44},$$
$$E^{2,3,4}-E_{\rm c.g.}=-\Xi_\mu T/9c_{44}, \tag{A13}$$

and the valley-orbit term becomes

$$-H_{\rm vo}{}^{s[111]}=\Delta_c\begin{vmatrix}-4/3x&1&1&1\\ 1&4/9x&1&1\\ 1&1&4/9x&1\\ 1&1&1&4/9x\end{vmatrix}, \tag{A14}$$

so that for valley populations $(\alpha_1,\alpha_2,\alpha_2,\alpha_2)$

$$E/\Delta_c=-4x/3+3\alpha_2/\alpha_1=4x/9-2+\alpha_1/\alpha_2. \tag{A15}$$

The solutions for the valley populations are then

$$\alpha_1{}^2=\tfrac{1}{4}\{2-[1-8x/9]\times[1+4x/9+(4x/9)^2]^{-1/2}\},$$
$$\alpha_2{}^2=(1/12)\{2+[1-8x/9]\times[1+4x/9+(4x/9)^2]^{-1/2}\}. \tag{A16}$$

For the ratio of hyperfine splitting under strain to unstrained value we get

$$|\psi_{(0)}|_s{}^2/|\psi_{(0)}|_i{}^2=\tfrac{1}{2}\{1+[1+2x/9]\times[1+4x/9+(4x/9)^2]^{-1/2}\}. \tag{A17}$$

The position of the singlet and admixed triplet states are given by

$$E^{e,f}/\Delta_c=-1-4x/9\pm2[1+4x/9+(4x/9)^2]^{1/2}. \tag{A18}$$

The other triplet levels with valley populations $(0, \alpha, -\alpha, 0)$ and $(0, \alpha, \alpha, -2\alpha)$ are degenerate and have energy given by

$$E^{g,h}/\Delta_c=1-4x/9. \tag{A19}$$

APPENDIX B: (g SHIFT UNDER STRAIN)

1. [110] Uniaxial Stress

For an electron in a single jth valley write with respect to *valley axis*

$$\mathbf{g}^{(j)}=\begin{vmatrix}g_\perp&0&0\\ 0&g_\perp&0\\ 0&0&g_{\rm II}\end{vmatrix}; \tag{B1}$$

in [100] frame write

$$\mathbf{g}^{(j)}=\begin{vmatrix}g_{11}&g_{12}&g_{13}\\ g_{21}&g_{22}&g_{23}\\ g_{31}&g_{32}&g_{33}\end{vmatrix}, \tag{B2}$$

where for H along $\langle111\rangle$ we get $g_j=g_{\rm II}$ and for H along $\langle1\bar10\rangle$ we get $g^{(j)}=g_\perp$. Solving, we find

$$g^{(j)}=\begin{bmatrix}g_0&\Delta_g&\Delta_g\\ \Delta_g&g_0&\Delta_g\\ \Delta_g&\Delta_g&g_0\end{bmatrix}\quad\begin{matrix}\Delta_g=\frac{1}{3}(g_{\rm II}-g_\perp)\\ g_0=(g_{\rm II}+2g_\perp);\end{matrix} \tag{B3}$$

averaging over the four valleys, without strain

$$g=[\sum(\alpha_j)^2(g^{(j)})]=g_0=\tfrac{1}{3}g_{\rm II}+\tfrac{2}{3}g_\perp. \tag{B4}$$

For g with [110] uniaxial compression, write

$$g^{(j)}=g_0\begin{bmatrix}1&0&0\\ 0&1&0\\ 0&0&1\end{bmatrix}+\Delta_g\begin{bmatrix}0&1&1\\ 1&0&1\\ 1&1&0\end{bmatrix} \tag{B5}$$
$$=g_0\mathbf{1}+\Delta_g\mathbf{U}^{(j)};$$

then

$$\mathbf{S}\cdot\mathbf{g}\cdot\mathbf{H}=\mathbf{S}\cdot[2(\alpha_1^2+\alpha_2^2)g_0\mathbf{1}+\Delta_g\sum\alpha_j^2\mathbf{U}^{(j)}]\cdot\mathbf{H}$$
$$=\mathbf{S}\cdot\left[g_0\mathbf{1}+\Delta_g(4\alpha_1^2-1)\begin{bmatrix}0&1&0\\1&0&0\\0&0&0\end{bmatrix}\right]\cdot\mathbf{H}. \quad \text{(B6)}$$

If we take as principal axes $\langle 110\rangle\langle 1\bar{1}0\rangle$ and $\langle 001\rangle$ then

$$\mathbf{S}\cdot\mathbf{g}\cdot\mathbf{H}=\mathbf{S}\cdot\begin{bmatrix}g_0+\Delta_g'&0&0\\0&g_0-\Delta_g'&0\\0&0&g_0\end{bmatrix}\cdot\mathbf{H}, \quad \text{(B7)}$$

$$\Delta_g'=\Delta_g(4\alpha_1^2-1). \quad \text{(B8)}$$

If one looks in the $[001]$–$[1\bar{1}0]$ plane, then

$$g^2=g_0^2[1+\{(\Delta_g'/g_0)^2-2(\Delta_g'/g_0)\}\sin^2\theta]. \quad \text{(B9)}$$

Solving for g and expanding

$$g/g_0=1-\sin^2\theta(\Delta_g'/g_0)+(\Delta_g'/g_0)^2(\tfrac{1}{2}\sin^2\theta-\tfrac{1}{2}\sin^4\theta)$$
$$+\text{terms in }(\Delta_g'/g_0)^3. \quad \text{(B10)}$$

For small values of strain ($x\leq 1$) we get upon substituting for α_1^2:

$$g-g_0=\frac{g_{11}-g_\perp}{3}\frac{x}{3(1+x^2/9)^{1/2}}\sin^2\theta. \quad \text{(B11)}$$

2. [111] Uniaxial Stress

Starting from the expression (B6) if we take the valley in the direction of the stress as U', we have

$$U'=\begin{bmatrix}0&1&1\\1&0&1\\1&1&0\end{bmatrix}, \quad \text{(B12)}$$

and the term

$$\sum_{j=1}^{4}\alpha_j\mathbf{U}^{(j)}=(\alpha_1^2-\alpha_2^2)\mathbf{U}', \quad \text{(B13)}$$

and

$$\mathbf{S}\cdot\mathbf{g}\cdot\mathbf{H}=\mathbf{S}\cdot\begin{bmatrix}g_0&\Delta_g''&\Delta_g''\\\Delta_g''&g_0&\Delta_g''\\\Delta_g''&\Delta_g''&g_0\end{bmatrix}\cdot\mathbf{H}, \quad \text{(B14)}$$

$$\Delta_g''=(\alpha_1^2-\alpha_2^2)\Delta_g. \quad \text{(B15)}$$

Taking as principal axes $\langle 111\rangle$, $\langle 1\bar{1}0\rangle$, and $\langle 11\bar{2}\rangle$, this matrix reduces to

$$\mathbf{S}\cdot\begin{bmatrix}g_0+2\Delta_g''&0&0\\0&g_0-\Delta_g''&0\\0&0&g_0-\Delta_g''\end{bmatrix}\cdot\mathbf{H}. \quad \text{(B16)}$$

If H moves in the plane formed by $\langle 11\bar{2}\rangle$ and $\langle 111\rangle$ axes

$$g^2=(g_0+2\Delta_g'')^2\cos^2\varphi+(g_0-\Delta_g'')\sin^2\varphi, \quad \text{(B17)}$$

where φ is the angle between H and $\langle 111\rangle$, or

$$g^2=g_0^2+2\Delta_g''^2$$
$$+(2\Delta_g''g_0+\Delta_g''^2)(\sin^2\theta+2\sqrt{2}\sin\theta\cos\theta) \quad \text{(B18)}$$

for θ with respect to $[100]$ axis in that plane.

3. To Calculate Line Broadening Due to g Shift

Assume only the average Gaussian component Δs of strain along the $[111]$ axis is important, as these give largest effect for small angles to the $[100]$ direction and small Δs.

$$g^2\cong g_0^2+2\Delta_g''g_0(\sqrt{2}\sin 2\theta). \quad \text{(B19)}$$

Solving for g and expanding, we get

$$\delta g=g-g_0\cong\sqrt{2}\Delta_g''/g_0\sin 2\theta. \quad \text{(B20)}$$

Substituting in the expression for Δ_g'', the valley populations α_1, α_2 for a $[111]$ compression, we have

$$\Delta_g''=(\alpha_1^2-\alpha_2^2)\Delta_g=(\Delta_g/3)\{1-[1-8x/9]$$
$$\times[1+4x/9+(4x/9)^2]^{1/2}\} \quad \text{(B21)}$$

for small compressive strains $|x|\ll 1$. This reduces to

$$\Delta_g''\cong(2x/9)\Delta_g.$$

Since the spread in H values ΔH^* is given by

$$\Delta H^*=(\delta g/g_0H),$$

we have

$$\Delta H^*=\frac{2\sqrt{2}}{27}\frac{g_{11}-g_\perp}{g_0^2}H\frac{\Xi_\mu}{E_{13}}\Delta s\sin 2\theta. \quad \text{(B22)}$$

APPENDIX C: LINEWIDTH FROM Ge^{73} INTERACTIONS

Kohn has derived the expression for the linewidth of the localized donor line as

$$\Delta H=\frac{32\pi}{3g}\frac{\mu_{Ge}}{I_{Ge}}\langle m_l^2\rangle_{av}^{1/2}[\sum_l n_l|\psi(r_l)|^4]^{1/2}. \quad \text{(C1)}$$

For the singlet ground state

$$\psi_{(r_l)}=\tfrac{1}{2}\sum_{j=1}e^{i\mathbf{k}_j\cdot\mathbf{r}_l}u(r_l)F^j(r_l). \quad \text{(C2)}$$

We will assume an isotropic form for the $F(r)$:

$$F(r)=\frac{1}{(\pi a_0{}^{*3})^{1/2}}e^{-r/a_0{}^*}, \quad \text{(C3)}$$

where

$$a_0{}^*=(E_{\text{eff mass}}/E_{\text{obs}})^{1/2}a_0=n(a^2b)^{1/3}. \quad \text{(C4)}$$

Expanding the sum above,

$$\sum_l n_l|\psi(r_l)|^4$$
$$=\frac{f\eta^2}{24(\pi a_0{}^{*3})^2}\sum_l n_l e^{-4r_l/a_0{}^*}|\sum_{j=1}e^{i\mathbf{k}_j\cdot\mathbf{r}_l}|^4, \quad \text{(C5)}$$

where

$|\sum e^{i\mathbf{k}_j\cdot\mathbf{r}_l}|$ = (256) for the simple cubic lattice positions, i.e., [400], [440], [444], etc.,
= 0 for the face-centered position such as [220], [422], etc.,
= (16) for all atoms on the displaced face-centered lattice, i.e., [111], [311], [333].

As a first approximation to the sum in (C5), one can simply integrate over the simple cubic lattice points, in which case

$$\sum_l n_l e^{-4r_l/a_0^*} = \int_0^\infty \frac{4\pi}{a_l^3} r^2 e^{-4r/a_0^*} dr \tag{C6}$$

$$= \frac{\pi}{8}\left(\frac{a_0^*}{a_l}\right)^3. \tag{C7}$$

To correct for the neglect of all the displaced face-centered lattice atoms we note there are four times as many atoms that contribute in that lattice, so that we correct the above sum to account for these times.

$$\sum n_l e^{-4r_l/a_0^*} = \frac{\pi}{8}\left(1+\frac{4\cdot 16}{256}\right)\left(\frac{a_0^*}{a_l}\right)^3 \tag{C8}$$

substituting this gives us finally

$$\Delta H = \frac{36}{3g}\frac{\mu_{Ge}}{I_{Ge}}\langle m_l^2\rangle_{av}^{1/2} f^{1/2}\eta \frac{1}{(a_0^* a_l)^{3/2}}. \tag{C9}$$

Kohn has also given an expression for the sum

$$S_{(\mathbf{k}_j)} = \sum_l n_l F^4_{(r_l)} \left|\sum_{j=1} e^{i\mathbf{k}_j\cdot\mathbf{r}_l}\right|^4 \tag{C10}$$

$$= \sum n_\alpha \left(\sum_l f(r_l) e^{i\mathbf{h}_\alpha\cdot\mathbf{r}_l}\right), \tag{C11}$$

where

$$f(r_l) = F^4(r_l)$$

and

$$\sum_\alpha n_\alpha e^{i\mathbf{h}_\alpha\cdot\mathbf{r}_l} = \left|\sum_{j=1} e^{i\mathbf{k}_j\cdot\mathbf{r}_l}\right|^4. \tag{C12}$$

Although $\sum n_\alpha = 4^4 = 256$, only five essentially different $\mathbf{h}_\alpha$ appear. These are

$$\begin{array}{lccccc} \mathbf{h}_\alpha = & (\pi/a_l)[0,0,0], & (\pi/a_l)[4,0,0], & (\pi/a_l)[4,4,0], & & \\ n_\alpha & 28 & 24 & 12 & & \\ & & & & (\pi/a_l)[2,2,0], & (\pi/a_l)[4,2,2]. \\ & & & & 144 & 48 \end{array}$$

In terms of these reciprocal lattice vectors, Kohn writes for the sum $S_{(\mathbf{k}_j)}$ using the Poisson sum rule,

$$S_{(\mathbf{k}_j)} = \frac{1}{2\pi(a_0^* a_l)^3}\sum_\alpha n_\alpha [e^{i\mathbf{K}_n\cdot\mathbf{A}_1}+1] \times\left[1+|\mathbf{K}_n-\mathbf{h}_\alpha|^2\cdot\left(\frac{a_0^*}{4}\right)^2\right]^{-2}. \tag{C13}$$

In this sum, essentially, only those terms contribute for which $\mathbf{K}_n = \mathbf{h}_\alpha$, since $(\mathbf{K}_n\cdot\mathbf{a}_0^*/4)\ll 1$ as the wave function spreads over many lattice spaces. Among the $\mathbf{h}_\alpha$, only the terms $\pi/a_l[000]$, $\pi/a_l[440]$, $\pi/a_l[400]$ appear in the body-centered reciprocal lattice and the last term does not contribute to the sum, i.e., so

$$S = \frac{1}{2\pi(a_0^* a_l)^3}\{80\}. \tag{C14}$$

Using this result, we find for ΔH

$$\Delta H = \frac{36}{3g}\frac{\mu_{Ge}}{I_{Ge}}\langle m_l^2\rangle_{av}^{1/2} f^{1/2}\frac{\eta}{(a_0^* a_l)^{3/2}}, \tag{C15}$$

i.e., the same result as obtained previously (C9).

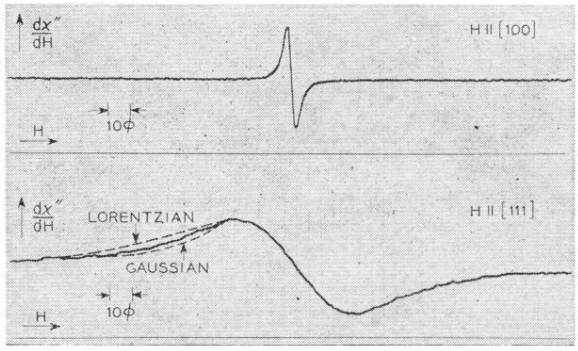

FIG. 17. Spin resonance spectrum for arsenic donors in germanium, $N_d = 6 \times 10^{16}/\text{cm}^3$ showing the motionally narrowed line shapes for magnetic field along [100] and [111] directions. $T = 1.2°\text{K}$, $H \sim 4000$ Oe. The line shape in [100] direction is very nearly Lorentzian while that in the [111] direction is more nearly Gaussian. This sample had a dislocation density $= 2 \times 10^4$ ϵ/cm^2.

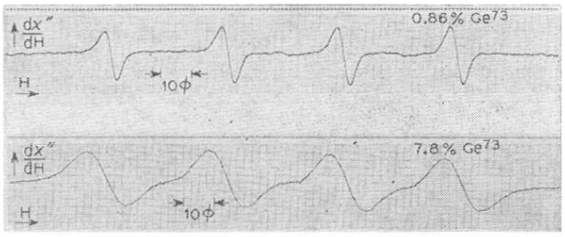

FIG. 3. Comparison of the spectrum for arsenic donors in isotopically enriched germanium, (0.86% Ge^{73}) and normal germanium (7.8% Ge^{73}), $T=1.2°K$, $H=4000$ Oe. Magnetic field along the [100] crystal axis, $N_d \cong 2\times10^{15}/cm^3$.

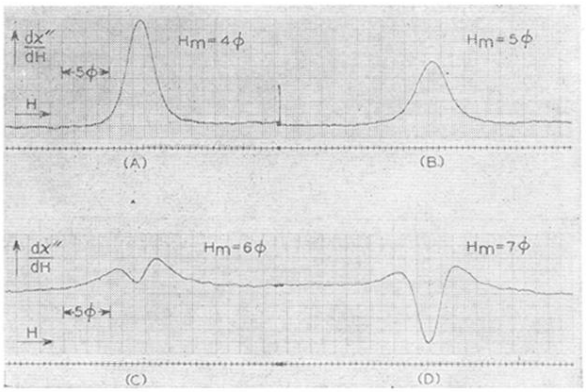

FIG. 9. Relative amplitude of the in-phase dispersion derivative versus magnetic field for increasing modulation amplitude (decreasing saturation) in isotopically enriched arsenic-germanium. The behavior of the dispersion signal indicates that the spin system is not able to recover completely between successive passages of the magnetic field.